

Selection of Summary Statistics for Network Model Choice with Approximate Bayesian Computation

Louis Raynal

Department of Biostatistics

T.H. Chan School of Public Health, Harvard University

655 Huntington Avenue, Building 2, 4th Floor

Boston, MA, USA 02115

lcraynal@hsph.harvard.edu

Jukka-Pekka Onnela

Department of Biostatistics

T.H. Chan School of Public Health, Harvard University

655 Huntington Avenue, Building 2, 4th Floor

Boston, MA, USA 02115

Abstract

Approximate Bayesian Computation (ABC) now serves as one of the major strategies to perform model choice and parameter inference on models with intractable likelihoods. An essential component of ABC involves comparing a large amount of simulated data with the observed data through summary statistics. To avoid the curse of dimensionality, summary statistic selection is of prime importance, and becomes even more critical when applying ABC to mechanistic network models. Indeed, while many summary statistics can be used to encode network structures, their computational complexity can be highly variable. For large networks, computation of summary statistics can quickly create a bottleneck, making the use of ABC difficult. To reduce this computational burden and make the analysis of mechanistic network models more practical, we investigated two questions in a model choice framework. First, we studied the utility of cost-based filter selection methods to account for different summary costs during the selection process. Second, we performed selection using networks generated with a smaller number of nodes to reduce the time required for the selection step. Our findings show that computationally inexpensive summary statistics can be efficiently selected with minimal impact on classification accuracy. Furthermore, we found that networks with a smaller number of nodes can only be employed to eliminate a moderate number of summaries. While this latter finding is network specific, the former is general and can be adapted to any ABC application.

Keywords: Approximate Bayesian Computation; summary statistic selection; mechanistic network models; classification; cost-based filter feature selection.

1 Introduction

In many areas of statistics, as data grow in dimension or become more complex, it becomes harder to handle the model likelihood which may be difficult to evaluate or it may not have a closed-form. This problem of intractable likelihood prevents the use of classic inferential techniques. Nonetheless, the stochastic process behind the data generation is often well understood, such that it is easy to simulate data given some parameter values. This is the cornerstone of a category of likelihood-free methods known as Approximate Bayesian Computation (ABC).

ABC can handle Bayesian parameter inference, as well as model selection problems, by approximating the posterior distribution of interest. The most basic ABC method is a rejection-sampling algorithm where (i) parameter samples are drawn from the prior distribution and (ii) data are simulated from the model conditional on these samples. If the *similarity* between the simulated and observed data is *high enough*, the sampled parameter is retained to form the approximated ABC posterior. *Similarity* is usually quantified by the distance between summary statistics of the data, with a distance threshold ϵ dictating which parameter values are accepted and which

are rejected. How to choose the distance, threshold, and summary statistics are the main questions when employing ABC and a tremendous amount of work continues to address these challenges [see e.g., [Blum, 2010](#), [Nunes and Balding, 2010](#), [Fearnhead and Prangle, 2012](#), [Prangle, 2017](#)]. Nonetheless, from its earliest application in population genetics to infer coalescent model parameters [[Pritchard et al., 1999](#)], ABC is now being applied in a wide variety of domains such as epidemiology [[Rodrigues et al., 2018](#)], systems biology [[Liepe and Stumpf, 2018](#)], climatology [[Holden et al., 2018](#)], ecology [[Fasiolo and Wood, 2018](#)], nuclear imaging [[Fan et al., 2018](#)], and population linguistics [[Thouzeau et al., 2017](#)]. A recent addition to this list is network science [[Dutta et al., 2018](#), [Chen et al., 2019](#), [Raynal et al., 2020](#)].

Networks are used to study interactions between elements, represented by nodes, and links between nodes are visualized as edges. The two main types of network model structure are based on statistical or mechanistic paradigms. The first model type relies on evaluation of the likelihood function, an example of which is the family of exponential random graph models [ERGM, [Lusher et al., 2013](#)]. The second type of model is defined by a small number of domain-specific rules, or mechanisms, informed by scientific knowledge. These rules are usually parameterized and used to mimic interactions between nodes to grow networks over time. Mechanistic models are therefore generative models, and because the growth history of a real network is usually unobserved, the likelihood function is intractable. As such, few statistically sound inferential methods are available for these models. ABC offers a good framework to fill this gap and has recently generated interest in the network science community. Examples of contributions are a general ABC-based framework for inference and model choice to study mechanistic models [[Onnela and Mira, In progress](#)], a flexible model selection approach for mechanistic network models [[Chen et al., 2019](#)], a Bayesian inference scheme for spreading processes on networks [[Dutta et al., 2018](#)], and recently, the use of extrapolated summary statistics to perform scalable ABC parameter inference [[Raynal et al., 2020](#)]. Mechanistic network models present important ABC questions: one of them is how to select summary statistics.

Summary statistic computation is a step included in most ABC techniques to ease the comparison between high-dimensional simulated and observed data. Even with this simplification, a small relevant set of summary statistics must be selected carefully to avoid the curse of dimensionality and ensure efficiency of the ABC algorithms [see e.g., [Prangle, 2018](#)]. However, an additional difficulty arises when studying large networks: evaluating certain summaries can be extremely time-consuming. For example, given a network with n nodes and m edges, the so-called betweenness centrality, a global measure of network connectivity, can be evaluated in time $O(n(m+n))$, while the number of triangles is trivially solvable in $O(n^3)$ [[Newman, 2010](#)]. Some other summary statistics, such as identification of network community structures [[Fortunato, 2010](#), [Traag et al., 2011](#)], can be non-deterministic polynomial-time (NP)-hard, requiring the use of heuristics for their evaluation. Therefore, evaluating summary statistics can create a computational bottleneck. Applying ABC techniques such as sequential Monte Carlo-ABC [[Sisson et al., 2009](#), [Del Moral et al., 2012](#)] can require millions of summary statistic evaluations. Reducing this computational burden by selecting summary statistics becomes even more critical for the study of networks.

A recent strategy to address ABC parameter inference or model choice problems involves using supervised machine learning (ML) algorithms trained on artificial datasets. These datasets, called *reference tables*, consist of simulated parameter values sampled from a prior distribution and associated data summary statistics values generated from the model. To learn the relationship between parameters and summary statistics, efficient regression/classification algorithms are employed such as deep neural networks [[Sheehan and Song, 2016](#)], [Breiman \[2001\]](#)'s random forest [[Pudlo et al., 2016](#), [Raynal et al., 2019](#), [Collin et al., 2020](#)], or the super-learner [[van der Laan et al., 2007](#), [Chen et al., 2019](#)]. Using such algorithms prevents the user from having to choose a distance and an acceptance threshold as they would in classic ABC strategies, while providing good prediction accuracy. The idea of using ML tools to solve ABC problems can be extended beyond parameter estimation and model choice, notably, to summary statistic selection. This subject is important even under the ML framework as the regression/classification algorithm may be sensitive to irrelevant summary statistics.

Summary statistic selection aims at avoiding the curse of dimensionality by determining a small set of relevant summary statistics. This challenging subject has received a lot of attention – see the book chapter of [Prangle \[2018\]](#) – but prior work has mostly been oriented toward parameter inference. Here, we focus on model choice problems by investigating the utility of ML feature selection methods to reduce the number of summary statistics. Note that, starting from a large set of potentially relevant summary statistics, we aim to select rather than extract them. Indeed, an extraction method builds new summaries, whereas a selection algorithm is restricted to the summaries initially computed. To our knowledge, very few ABC papers have made use of ML tools to select summary

statistic subsets. For example, [Estoup et al. \[2012\]](#) trained a linear discriminant analysis to determine relevant combinations of raw data that were then taken as summary statistics. This work falls into the category of summary statistic extraction methods, not selection. For parameter inference, [Sedki and Pudlo \[2012\]](#) and [Blum et al. \[2013\]](#) proposed to select a subset of summary statistics using the AIC or BIC when training a linear regression between parameters and summaries.

Because the analysis of mechanistic network models is our main concern, we investigated strategies able to handle the computational bottleneck that can occur when computing network summary statistics. In this setting, we explored two strategies to select summary statistic subsets efficiently. First, we focused on feature selection methods that take into account each summary statistic’s computational time. These *cost-based* methods identify a set of relevant summary statistics that are fast to compute. Second, to reduce the computational cost of the selection process, we used summary statistics based on smaller graphs with fewer nodes than the observed one. While this second approach is restricted to mechanistic network models, the first one relies on cost-based algorithms and thus is general and can be applied to any field. We analyzed these approaches using two simulated classification problems, one based on the Barabási–Albert model [\[Barabási and Albert, 1999\]](#) and the other to discriminate between two protein-protein interaction network models: the Duplication Mutation Complementation model [\[Vázquez et al., 2003\]](#) and the Duplication with Random Mutation model [\[Solé et al., 2002\]](#).

In this paper, we start with a description of the model choice setting, including the generation of a reference table and the different methods that will be used on it (Section 2). With the two simulated classification problems, we illustrate the utility of the cost-based algorithms (Section 3). We then compare the relevance of the summary statistics computed on small and large networks (Section 4), and discuss the results (Section 5).

2 Materials and methods

2.1 Reference table and feature selection

First, we formalized the ABC model choice setting. We considered a problem with M (mechanistic network) models, and determined which model would most likely give rise to the observed data $\mathbf{y}_{\text{obs}} \in \mathcal{Y}$. The parameter of interest was therefore the model index \mathcal{M} , to which we assigned a prior probability mass function: $\{\mathbb{P}(\mathcal{M} = m)\}_{m=1, \dots, M}$. Each model indexed by m , in addition to its prior probability, had its own parameters $\boldsymbol{\theta}_m$, which were assigned a prior distribution $\pi_m(\cdot)$. The intractable model likelihoods were $f_m(\cdot | \boldsymbol{\theta}_m)$, with $m \in \{1, \dots, M\}$. Given q potential summary statistics, denoted $\mathbf{s}(\mathbf{y}) := (s_1(\mathbf{y}), \dots, s_q(\mathbf{y})) \in \mathcal{F} \subseteq \mathbb{R}^q$ where \mathcal{F} is the summary statistic space, our objective was to select q' of those that were relevant to discriminate between the different models.

To select summary statistics, we simulated a reference table of size N , made of simulated model indices and corresponding q summary statistics. Algorithm 1 depicts the simulation process to obtain a reference table with N elements. When considering the model indices as responses and summaries as features, this table can be used to train a supervised classifier that will predict the model index for any set of summaries corresponding to a new observation. Using some clever tricks, it is even possible to retrieve the model posterior probabilities, see for example [Pudlo et al. \[2016\]](#) or [Chen et al. \[2019\]](#). However, the choice of classifier was not our main concern. We used this table to reduce the number of summaries by training a supervised feature selection method.

Algorithm 1: Generation of a reference table with N elements (rows)

```

for  $i \leftarrow 1$  to  $N$  do
    Generate  $m^{(i)}$  from the prior  $\mathbb{P}(\mathcal{M} = m)$ 
    Generate  $\boldsymbol{\theta}_{m^{(i)}}$  from the prior  $\pi_{m^{(i)}}(\cdot)$ 
    Generate  $\mathbf{y}^{(i)}$  from the model  $f_{m^{(i)}}(\cdot | \boldsymbol{\theta}_{m^{(i)}})$ 
    Compute  $\mathbf{s}(\mathbf{y}^{(i)}) = (s_1(\mathbf{y}^{(i)}), \dots, s_q(\mathbf{y}^{(i)}))$ ;
end

```

Supervised feature selection methods are well developed in the ML literature. They are commonly divided into three categories: *filter* methods, *embedded* methods, and *wrapper* methods [\[Jović et al., 2015\]](#). A *filter* method can be seen as a preprocessing feature selection step, independent of the learning algorithm. It determines the relevance of features using various measures such as correlation or mutual information [\[Shannon, 1948\]](#) rather than prediction accuracy. In contrast, a *wrapper*

directly uses the learning algorithm to evaluate the relevance of feature subsets in terms of prediction accuracy, for example. An *embedded* approach performs feature selection during the training of the learning algorithm, as in the case of random forests [Breiman, 2001] or LASSO [Tibshirani, 1996]. We focused on filter methods because we could use them as a preprocessing step before applying other selection techniques, and they are relatively fast compared to wrappers and embedded methods.

While any common filter selection algorithm can be utilized, studying large network datasets with ABC can be computationally difficult depending on the complexity of the summary statistics. To address this problem, we explored two independent strategies detailed below.

Cost-based filter selection method. When evaluating summaries, the time taken to compute them should be incorporated in the selection methods. Indeed, when two summaries are equally informative for the classification task, we would select the one that is less computationally intensive. In general, we wanted to create a balance between informativeness and computational cost. To this end, we adapted to our ABC problem a *cost-based* class of feature selection strategies.

Cost-based feature selection methods are fairly recent and found their first application in medicine. In this context, a feature consists of information on a patient and retrieving it carries a financial cost dependent on the nature of the feature (e.g., X-ray image vs. PET scan, where the latter is approximately ten times more expensive than the former). The objective is to achieve a trade-off between total financial cost to obtain the features and their informativeness for the classification problem. In the filter category, Bolón-Canedo et al. [2014b] initially proposed an adaptation of the ReliefF algorithm [Kononenko, 1994] and then a more general framework adapting the correlation-based and minimal-redundancy-maximal-relevance criteria [Peng et al., 2005, Bolón-Canedo et al., 2014a]. Zhou et al. [2016] made use of a Breiman [2001]’s random forest where the feature cost is used at each internal node of a tree to sample inexpensive features more often than expensive ones. A recent wrapper proposal from Zhang et al. [2019] used an artificial bee colony algorithm for subset exploration. When imposing a total cost limitation (a.k.a., hard-margin), Jagdhuber et al. [2020] proposed a modified genetic algorithm as well as a greedy forward selection approach based on the Akaike Information Criterion. Our goal with such methods was to select a subset of summaries with low computational cost that do not alter the accuracy of the classifier compared to the version that ignores cost.

To apply cost-based methods in our summary selection framework, we first needed to substitute the financial cost with the computation time necessary to evaluate the different summaries. To determine this cost, when generating a reference table with N elements, we kept track of the computation time required to evaluate each summary for each simulation. For a given summary, we averaged these times over all simulations to obtain its cost. Therefore, the vector of averaged summary times was our cost vector (C_1, \dots, C_q) . This is the expected computation time to calculate the different summaries of randomly simulated data. Other measures can also be used, such as the maximum or the median of the individual times. However, the former depends only on the densest simulated networks, while the latter would ignore their impact. In the following, we rescaled our vector of cost so that each element was bounded between 0 and 1, with the total cost equal to 1 when no selection was performed. This meant that the cost of a summary statistic subset would always be a proportion of the total cost, highlighting the potential cost reduction obtainable when performing selection.

Furthermore, to avoid biasing selection toward summaries that can be computed in groups, we evaluated all features independently without recycling information used by a given summary evaluation to compute another. This is, for example, the case of moments of the degree distribution, for which multiple moments (i.e., summaries) can be determined using only one evaluation of the degree density.

Feature selection with small networks. The inferential scheme of our paper includes two reference tables. One contains q summaries that we used for feature selection, and the other contains $q' < q$ summaries used to train a classifier. Both were obtained from network data generating up to n_o nodes, the number of nodes in the observed network. For a large value of n_o , generating the first table can be very expensive depending on the value of q , so we reduced its generation time by reducing the sizes of the simulated networks. We stopped the simulation process at n_s nodes, with $n_s < n_o$, to form the table used to adjust a classic feature selection algorithm. In this way, we investigated whether summary statistics selected to classify smaller networks remain relevant for classifying larger ones.

As previously noted, mechanistic models generate networks by sequentially adding nodes to a small seed graph according to a given mechanism until n_o nodes are present. Here, our strategy

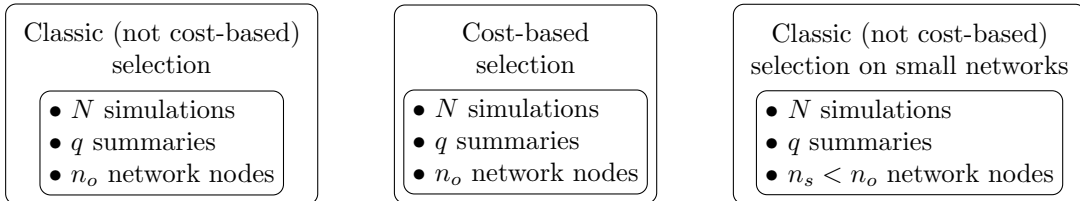


Figure 1: Three versions of summary statistic selection frameworks evaluated in this paper. We investigated the use of cost-based selection techniques and the utility of small networks.

of using smaller networks can be interpreted as stopping network construction early to assess the ability of the associated summaries to distinguish between the different models.

Figure 1 recaps the summary selection settings discussed so far, as well as the characteristics of the reference table for this purpose. We studied the classic selection problem indirectly, as it is a special case of cost-based selection.

We used the following filter methods and their possible cost-based counterparts. The three typical categories we considered are based on mutual information [Shannon, 1948], the ReliefF algorithm [Kira and Rendell, 1992, Urbanowicz et al., 2018a], and random forest feature importance [Breiman, 2001]. Again, these are general selection methods and not network specific.

To avoid confusion, when presenting the feature selection methods, we adopted the standard notation of supervised learning. We considered a classification problem where the response variable Y takes values in a finite set $\{1, \dots, M\}$, and the vector of covariates is denoted by $X = (X_1, \dots, X_q)$. The training dataset consisted of N independent realizations $(y^{(i)}, \mathbf{x}^{(i)})$ of (Y, X) . In our application, the response was our model index, and the summary statistics were the network features.

2.2 Mutual Information-based approaches

Shannon [1948]’s Mutual Information (MI) is a relevant measure for feature selection because it quantifies the amount of information that one variable carries about another. Given two discrete random variables X_1 and X_2 with values in the sets \mathcal{X}_1 and \mathcal{X}_2 , respectively, their mutual information is defined as

$$I(X_1; X_2) = \sum_{x_1 \in \mathcal{X}_1} \sum_{x_2 \in \mathcal{X}_2} p(x_1, x_2) \log \left(\frac{p(x_1, x_2)}{p(x_1)p(x_2)} \right),$$

where $p(\cdot)$ and $p(\cdot, \cdot)$ respectively denote the univariate and joint probability mass functions. (Note that this expression is symmetric.) While the mutual information quantifies the relevance of a feature with respect to another, an additional quantity of interest is the conditional mutual information $I(X_1; X_2 | X_3)$, where X_3 is a third discrete random variable with values in the set \mathcal{X}_3 . It measures the information between two features conditionally to the knowledge of a third one. Its expression is

$$I(X_1; X_2 | X_3) = \sum_{x_3 \in \mathcal{X}_3} p(x_3) I(X_1; X_2 | X_3 = x_3),$$

where $I(X_1; X_2 | X_3 = x_3)$ is the mutual information computed on the data subset where $X_3 = x_3$.

All the following feature selection methods based on MI are sequential forward methods, where the feature subset is empty at the start and features are sequentially selected and added to it, one at a time. In other words, at the l -th step, $l - 1$ features are already selected, and the newly selected X_k is the one that maximizes an evaluation function $J(X_k)$. Various forms for $J(\cdot)$ can be adopted. Below we describe three of these methods that are of particular interest and commonly used.

Minimal-Redundancy-Maximal-Relevance

The minimal-redundancy-maximal-relevance method [mRMR, Peng et al., 2005] relies on the evaluation function

$$J_{\text{mRMR}}(X_k) = I(X_k; Y) - \sum_{j \in \mathcal{S}} I(X_j; X_k), \quad (1)$$

where \mathcal{S} designates the set of feature indices already selected. As its name suggests, the first term corresponds to a relevance expression, while the second corresponds to the redundancy between a new candidate feature X_k and the features already selected.

Joint Mutual Information

Yang and Moody [1999] proposed to use the joint mutual information $I((X_j, X_k); Y)$ (JMI) method. JMI describes the information between a pair of features, jointly considered together, and the response. The evaluation function when applied to a potential feature X_k is

$$J_{\text{JMI}}(X_k) = \sum_{j \in \mathcal{S}} I((X_j, X_k); Y). \quad (2)$$

Interestingly, this criterion can be transformed equivalently (in the sense that it does not change the maximization process, see Brown et al. [2012]) into

$$J_{\text{JMI}}(X_k) \propto I(X_k; Y) - \sum_{j \in \mathcal{S}} I(X_j; X_k) + \sum_{j \in \mathcal{S}} I(X_j; X_k | Y), \quad (3)$$

which is the mRMR criterion plus a positive term for the MI between the X_j 's and X_k conditional on Y . Thanks to this term, the JMI criterion is able to detect positive interactions between features with respect to the response. As highlighted by Brown et al. [2012], while the terms $I(X_j; X_k)$ are negatively signed to reduce the correlation/redundancy between features, the conditional MI terms are positively signed, thus “the inclusion of correlated features can be useful, provided the correlation within classes is stronger than the overall correlation” [Brown et al., 2012].

Joint Mutual Information Maximization

As an alternative method proposed by Bennasar et al. [2015], a “maximization of the minimum” (maximin) perspective is taken by replacing the sum with the minimum over all previously selected features in Equation (2). The criterion to maximize becomes

$$J_{\text{JMIM}}(X_k) = \min_{j \in \mathcal{S}} [I((X_j, X_k); Y)].$$

Similarly to $J_{\text{JMI}}(\cdot)$, this criterion is equivalent to

$$J_{\text{JMIM}}(X_k) \propto \min_{j \in \mathcal{S}} [I(X_k; Y) + I(X_j; Y) - I(X_k; X_j) + I(X_k; X_j | Y)]. \quad (4)$$

In our experiments, we kept track of the summary statistic types when necessary (discrete or continuous). For this reason, the second expressions (Equations (3) and (4)), which might seem more complicated, are actually more practical when continuous and discrete covariates need to be evaluated jointly. Indeed, the mutual information is originally defined for either discrete or continuous variables, and adaptations have been proposed to evaluate $I(X_j; X_k)$ when one covariate is discrete and another continuous [see e.g., Ross, 2014]. However, when evaluating the JMI $I((X_j, X_k); Y)$, it is not obvious how to proceed when only one of the two features is continuous. At the bare minimum, when both are continuous, we could discretize values using bins, but binning is less natural when the joint distribution (X_j, X_k) is discrete-continuous. For a discrete Y , the terms of the alternative expressions (3) and (4) can be easily evaluated individually with current strategies regardless of the covariate types.

Cost-based versions

The cost-based versions of these filter selection methods are easily constructed by penalizing the evaluation functions of X_k (previously defined in Equations (1), (3), and (4)) by its cost C_k . In other words, the new evaluation function is expressed as

$$J(X_k) - \lambda C_k,$$

where λ is a positive parameter that dictates the balance between the relevance of a feature and its cost. The mRMR adaptation is introduced by Bolón-Canedo et al. [2014b], but the JMI and JMIM adaptations are new and interesting for their potential to handle positive interactions among features.

Interestingly, Brown et al. [2012] unified a large number of MI-based feature selection criteria. Starting from the maximization of the conditional likelihood of the labeled data, they showed that most classic criteria can be recovered by assuming low-order approximations of the exact maximization problem. Interestingly, starting from the same conditional likelihood that we penalize by $\lambda \sum_{j \in \mathcal{S}} C_j$, we can similarly derive the penalized criteria (1) and (3), assuming the same approximations in terms of feature dependency.

2.3 ReliefF-based approaches

The second category of filter selection methods we used is ReliefF [Kononenko, 1994], a multi-class extension of the original Relief algorithm of Kira and Rendell [1992]. It is a ranking selection algorithm that determines a weight (or score) for each feature that increases with its importance. The general idea behind Relief-based methods is to quantify the relevance of a feature based on how well it separates data with different labels and how close data with identical labels are from each others.

Algorithm 2 describes the ReliefF algorithm. At each of its iterations, a labeled data point $R^{(i)} := (y^{(i)}, \mathbf{x}^{(i)})$ (a.k.a., instance) is randomly selected without replacement and its ℓ nearest neighbors within each class are identified. The neighbors within the same class are called “hits” and those in different classes are called “misses.” Each feature weight is updated based on the following rule: a feature that is relevant for distinguishing between classes should result in high distances between $R^{(i)}$ and its misses—when projected onto this dimension—since they have different labels. At the same time, the distances between $R^{(i)}$ and its hits should be small since they have the same label. This second criterion leads to a negative term on the weight update expression, while the first leads to a positive term. The algorithm cycles r times through the process of selecting a random instance $R^{(i)}$ and updating weights. In our experiments, as proposed by Urbanowicz et al. [2018b], each training instance was selected successively (i.e., $r = N$ without randomization). A common choice for the number of nearest hits and misses that provides good performance is $\ell = 10$ [Urbanowicz et al., 2018a], so we used this value in our analysis. The distance between two instances $R^{(1)}$ and $R^{(2)}$ on the u -th covariate dimension is defined by

$$d_{X_u}(R^{(1)}, R^{(2)}) = \begin{cases} \frac{|x_u^{(1)} - x_u^{(2)}|}{\max(X_u) - \min(X_u)}, & \text{if } X_u \text{ is numeric,} \\ \mathbb{1}_{\{x_u^{(1)} \neq x_u^{(2)}\}}, & \text{if } X_u \text{ is nominal/categorical,} \end{cases}$$

where $\mathbb{1}$ denotes the indicator function. This distance is summed over all dimensions to determine the nearest neighbors.

Algorithm 2: ReliefF algorithm (not cost-based).

Initialize all feature weights $w(X_u)$ to zero;

for $i \leftarrow 1$ **to** r **do**

 Randomly select a target instance $R^{(i)}$;

 Find ℓ nearest hits $H^{(j)}$;

for each class $c \neq \text{class}(R^{(i)})$ **do**

 From class c find ℓ nearest misses $M^{(j)}(c)$;

end

for $u = 1$ **to** q **do**

$$w(X_u) = w(X_u) - \frac{1}{r \times \ell} \sum_{j=1}^{\ell} d_{X_u}(R^{(i)}, H^{(j)}) + \frac{1}{r \times \ell} \sum_{c \neq \text{class}(R^{(i)})} \left[\frac{p(c)}{1 - p(\text{class}(R^{(i)}))} \sum_{j=1}^{\ell} d_{X_u}(R^{(i)}, M^{(j)}(c)) \right]$$

end

end

Bolón-Canedo et al. [2014b] proposed a cost-based adaptation of ReliefF, by penalizing the weight update expression, leading to

$$w(X_u) = w(X_u) - \frac{1}{r \times \ell} \sum_{j=1}^{\ell} d_{X_u}(R^{(i)}, H^{(j)}) + \frac{1}{r \times \ell} \sum_{c \neq \text{class}(R^{(i)})} \left[\frac{p(c)}{1 - p(\text{class}(R^{(i)}))} \sum_{j=1}^{\ell} d_{X_u}(R^{(i)}, M^{(j)}(c)) \right] - \lambda \frac{C_u}{r}.$$

Note that the original proposal of Bolón-Canedo et al. [2014b] used $\lambda C_u / (r \times \ell)$ as penalization; however, we did not see much justification for the factor ℓ , so we discarded it to be more consistent across the different feature selection methods. Interestingly, this penalization is performed r times and does not depend on i . Therefore, we could equivalently apply a penalization by λC_u on the final feature weights returned by a classic ReliefF algorithm.

One issue with ReliefF is its sensitivity to noise features. Indeed, neighbors (hits and misses) are identified by computing distances over the complete feature space; however, noise features can misleadingly change the identity of the nearest neighbors and thus the final feature scores and ranking. To prevent this issue and possibly improve the quality of the selected features, we used a random forest to determine the similarity between pairs of training data when determining neighbors. We used the Breiman [2001]’s proximity matrix, whose entries denote the average number of times two data points fall in the same leaf, where the average is taken over all trees. The matrix is obtained by training a random forest using the model indices as responses, and the simulated network features (summary statistics) as explanatory variables. This similarity metric has the advantage of being based mostly on relevant features. To guarantee enough data with non-zero similarities, we built shallow trees, in the sense that we stopped their construction before each tree branch had fewer than 100 instances (training data) in it.

2.4 Random forest importance-based approaches

Finally, we considered filter selection methods based on random forest measures of importance to obtain a ranking of the features. Recall that a random forest (RF) is an ensemble of decision trees [CART, Breiman et al., 1984] whose construction is randomized by using bootstrap samples for each tree, and subsampling the covariates at each tree node. Random forests can be used to rank covariates based on their relevance for the learning task. Two measures of importance are commonly used: the mean decreased impurity (MDI) and the mean decreased accuracy (MDA) [Biau and Scornet, 2016]. A decision tree is built by sequentially partitioning the covariate space according to a covariate and a split value so that this cut maximizes an information gain criterion. The criterion is maximized only over a subset of the features; \sqrt{q} is a common default choice in classification and we used it in the following analysis. For a given feature, to compute the MDI, the information gain can be summed over all trees and all nodes where this feature has been used. The MDA of a feature is computed over all trees as the decrease in accuracy obtained on out-of-bag data when randomly permuting its covariate values, where out-of-bag data refers to a data point that is not selected in a given bootstrap sample and thus is not used to construct the given tree.

We examined two alternative cost-based variants. The first is a more flexible adaptation of the proposal by Zhou et al. [2016], while the second is a simple penalization of the MDI or MDA.

Weighted random forest adaptation

In the vanilla RF algorithm, at each internal node the information gain is maximized on a subset of features that are uniformly drawn at random. The proposal described by Zhou et al. [2016] consists of training a random forest by replacing the uniform sampling of covariates at each node of each tree by weighted sampling where expensive features are less likely to be selected. The forest then uses the resulting feature ranking (measured with the MDI or MDA) to determine which features to retain. The sampling weights are defined by the reciprocal of their cost, so that a feature u has sampling probability

$$w_u = \frac{1/C_u}{\sum_{i=1}^q 1/C_i}.$$

We proposed a simple generalization of this idea to generate sampling weights that depend on a tuning parameter λ similar to the other cost-based methods examined in this paper. This parameter was expected to drive the importance of cost relative to prediction accuracy. To maintain consistency with the original method of Zhou et al. [2016], we defined the weight of a given feature u as

$$w_u(\lambda) = \frac{1/C_u^\lambda}{\sum_{i=1}^q 1/C_i^\lambda}.$$

Introducing λ as the exponent of the costs allows a smooth transition between a classic (i.e., not cost-based) random forest algorithm when $\lambda = 0$ and the original strategy of Zhou et al. [2016] when $\lambda = 1$. While λ influences the cost of other methods through a multiplicative term, here the exponentiation has much greater impact on the final weights as λ grows. For this reason, in our experiments we considered a much smaller range of values for this parameter.

Penalized random forest feature importance

Finally, a more naive cost-based approach that benefits from the RF ranking consists of penalizing the random forest importance values from a forest built on a simulated reference table. We retrieved the feature importance measures (MDI or MDA), and after normalization between zero and one, we subtracted λC_u from each corresponding u -th feature importance. Normalization makes the two measures more comparable with each other for the same value of λ . This approach is similar to the cost-based ReliefF algorithm, as the cost impacts the ranking afterward.

We implemented all the presented cost-based methods in a Python package named `cost_based_selection`, see the Code availability Section.

3 Simulation studies: cost-based filter selection

We studied the efficiency of the cost-based filter selection methods presented in Section 2. We considered two simulation problems of network model choice: the first one classified four Barabási–Albert models, and the second involved two models that describe protein-protein interaction networks.

3.1 Barabási–Albert models

The Barabási–Albert (BA) model [Barabási and Albert, 1999] is a simple and influential mechanistic network model of undirected networks. It has two parameters we denoted as n_1 and n_2 . The first parameter is the final number of nodes in the network. The second parameter describes to how many existing nodes a new node will be connected. More precisely, starting from a small seed graph, at each step of the network growth, a new node is added and connected by n_2 edges to n_2 existing nodes selected by so-called preferential attachment. Preferential attachment dictates that a node is selected with probability proportional to its degree, so it describes the notion of “the rich get richer,” where high-degree nodes attract new neighbors faster than low-degree nodes. We used the BA model to define a simple four-class classification problem. We considered four possible values for n_2 , either 1, 2, 3, or 4, while n_1 remained fixed to a value equal to the observed number of nodes, $n_o = 1000$ for this example. For our simulation studies, we used the Python package `NetworkX` [Hagberg et al., Aug 2008] to generate networks. For the BA model, we used a small, fully connected graph of n_2 nodes as the seed network. In practice, this seed network may be selected based on certain characteristics or structures of the observed network, and/or is motivated by domain knowledge [see e.g., Hormozdiari et al., 2007, Schweiger et al., 2011].

For summary statistic selection, we obtained a reference table by simulating $N = 5000$ networks on which 58 summary statistics were evaluated. We generated the networks with equal proportions among the four settings described above, in other words, the model index carried a uniform probability. Note that the model index was, in fact, the parameter n_2 , and for this reason we did not have any other prior distribution. The 58 summaries are listed in Appendix A, Table 3. They include a wide variety of network features as well as four inexpensive noise covariates that represent independent realizations from four different distributions. These distributions are normal $\mathcal{N}(0, 1)$, uniform $\mathcal{U}_{[0, 50]}$, Bernoulli $\mathcal{Ber}(0.5)$, or discrete uniform $\mathcal{U}_{[0, 50]}$. Such irrelevant noise features were useful for studying the different selection strategies.

Because of the simplicity of the models, it was easy to discriminate among them. For a given BA model, certain summaries presented a unique modality and were thus extremely relevant for identifying the different models. This was true of the number of edges in the largest connected component (LCC) and in the whole network (these two were identical here), as well as the average degree. While these summary statistics were relevant, others were not since they did not vary with the model index and thus could not be used to identify the different models. These non-relevant summaries included the number of connected components, the number of nodes in the LCC, and the number of 5- and 6-cores/shells. We therefore discard them before training the cost-based methods. Using the feature selection algorithms we selected the 15 best summaries; in practice, this choice would be left to the user.

To assess the quality of the resulting subsets of summaries, since their selection was independent of the classifier, we used a second reference table of the same size $N = 5000$ built with the determined summaries. On this table, we performed a 3-fold stratified cross-validation to train and evaluate the prediction accuracy of an untuned Support Vector Machine (SVM) algorithm and a k -nearest neighbors classifier (k -NN) with $k = 10$. The use of this latter classifier was motivated by the fact that one can perceive the basic ABC algorithm as a k -NN algorithm [Biau et al., 2015]. While the

choice of the classifier is not the subject of this paper, employing the super-learner enables one to use a combination of various classifiers [van der Laan et al., 2007].

Figures 2 and 3 represent for each selection method and each λ value the evolution of three quantities: the prediction accuracy, the total cost of the selected summaries (1 being the cost without selection), and the proportion of selected noise features relative to the total number of noise features we introduced (hence 0%, 25%, 50%, 75% or 100%). Except for the weighted RF approach, the grid for λ ranged from 0 to 100, with a step of 0.02, to guarantee a sufficient decrease of the total cost. For the weighted RF, the grid only ranged from 0 to 2, with a step of 0.002, because of the high impact of this parameter on the RF covariate sampling.

Before detailing the results of these figures it is important to stress that even though the grids for λ might be the same, the curves obtained with different selection methods were not always pointwise comparable. Indeed, to compare the results of two cost-based strategies for the same λ value, it is necessary that their unpenalized criteria have the same range of values. For this reason, the cost-based mRMR, JMI, and JMIM methods could not be directly compared with one another. However, we did compare the results of the two versions of ReliefF, as well as the weighted RF and penalized RF importance.

In general, we noticed that both classifiers yielded high prediction accuracies, often close to 100%, even though the SVM was always inferior to the 10-NN. These accuracy measures tended to decrease when λ increased, and as intended, the total cost of the selected summaries decreased substantially. This was the expected behavior of these cost-based strategies as they try to select increasingly inexpensive features, to the detriment of their relevance. Nonetheless, a gain in accuracy was not impossible, especially if the classifier performance was already poor when $\lambda = 0$. Indeed, by increasing the value of λ , we explored additional subsets of summary statistics, which could improve low classification accuracy. This was notably the case for the ReliefF algorithms.

We observe in Figure 2 that the mRMR accuracy remained unchanged no matter the penalization value, but if the value of λ got too large, it led to the inclusion of one of the four noise features. Unsurprisingly, JMI and JMIM accuracies degraded when λ increased, with a drop of about 30% for the SVM. For JMI, we noticed that the total cost without penalization was already very low; furthermore, the accuracy of the SVM algorithm could result in very large confidence intervals. Concerning the ReliefF approaches, for $\lambda = 0$, the accuracies of the classifiers were not optimal and included all noise features. Moreover, the total costs of the summary subsets were surprisingly low. This suggests that the quality of the summaries selected by the not cost-based ReliefF methods was poor. However, we observed that increasing λ helped to reveal more relevant subsets that improved the classification accuracy while decreasing the total cost. Both versions of ReliefF (the classic and our proposed approach using RF proximity) behaved similarly and surprisingly included all noise features. Increasing the penalization parameter did not exclude these noise features since they had some of the lowest costs and were already included when $\lambda = 0$.

In Figure 3, the results for the weighted RF approaches with MDI and MDA were extremely similar. The total cost curves were very noisy compared to all other methods, highlighting a high variability in the top 15 features. This behavior originated in the additional randomness induced by the construction of a different random forest for each value of λ . Nonetheless, the cost tended to decrease, with excellent performance and while ignoring noise. Finally, the penalized RF importances also provided perfect accuracy with a high tolerance to noise, as well as a large decrease in cost.

The results of this example are very encouraging since they demonstrate that it is possible to find a value of λ that clearly decreases the average total feature cost, without decreasing the classification accuracy. The inclusion of cheap noise features can be a helpful way to determine an appropriate λ value since we could identify ranges of λ that led to exclusion of the noise features in the final summary statistic subset. Note that considering expensive noise would not have been useful, as these features are less likely to be included before the cheap ones when λ increases. This simple example resulted in nearly perfect predictions. We consider a more difficult scenario below.

3.2 Models for protein-protein interaction networks

To pursue our study of cost-based filter selection methods, we next focused on the classification of two mechanistic network models commonly used to describe protein-protein interaction networks: the Duplication Mutation Complementation (DMC) [Vázquez et al., 2003] and the Duplication with Random Mutation (DMR) [Solé et al., 2002] models. Even though we only considered two models, each has an intractable likelihood function and no summary completely identifies either of them.

For both models, each step of network generation starts by adding an unconnected node to the network. Then, a previously existing node is uniformly selected at random, and all its neighbors are

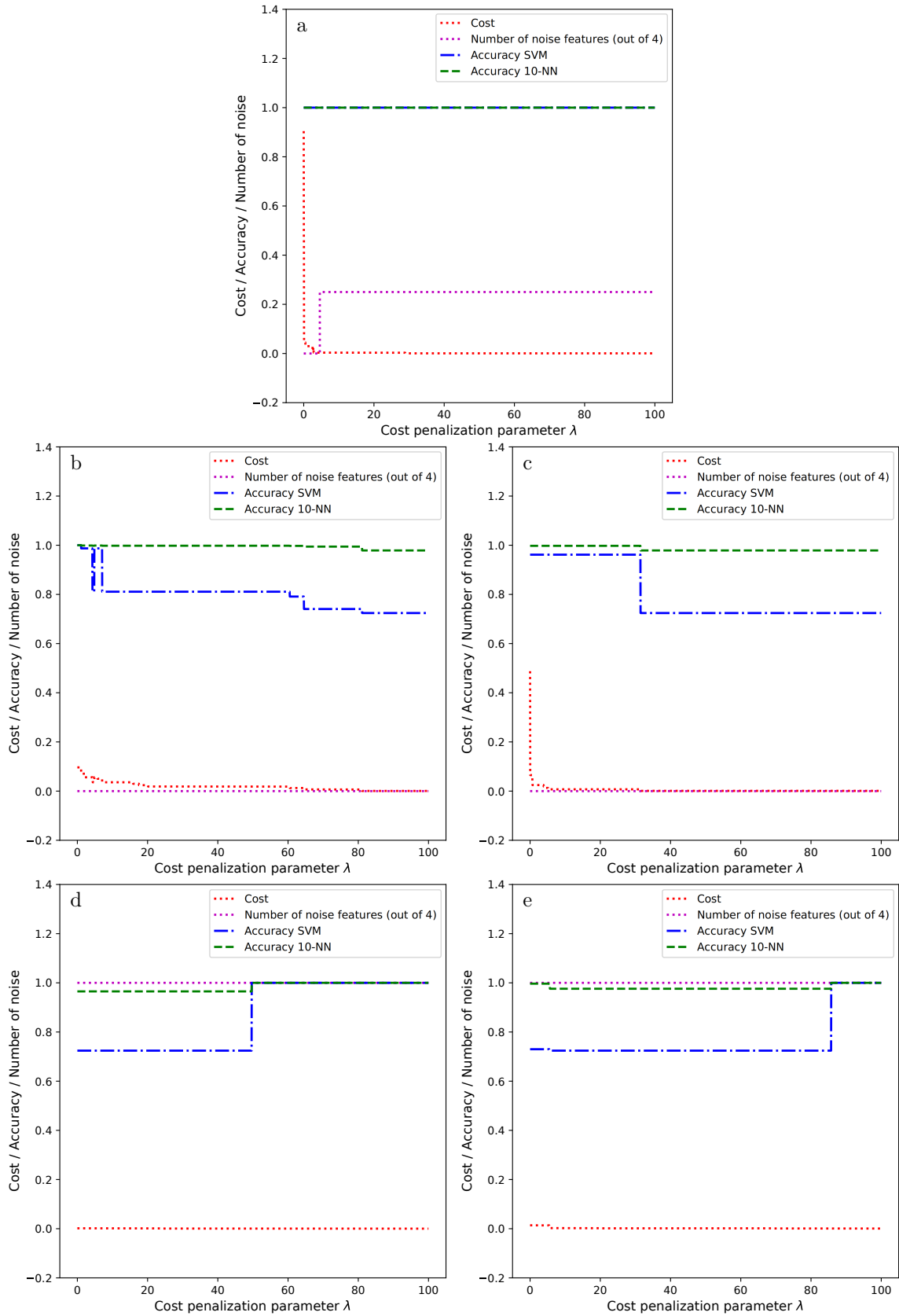


Figure 2: Evolution plots as a function of the penalization parameter value λ , of the accuracy of the SVM and 10-NN classifiers, total cost, and proportion of noise in the summary subsets determined by the mRMR (panel a), JMI (panel b), JMIM (panel c), and ReliefF-based algorithms (panel d for the classic version and panel e for the version using RF proximity matrix). These graphs relate to the selection of the four BA models. 15 summaries are selected out of 52.

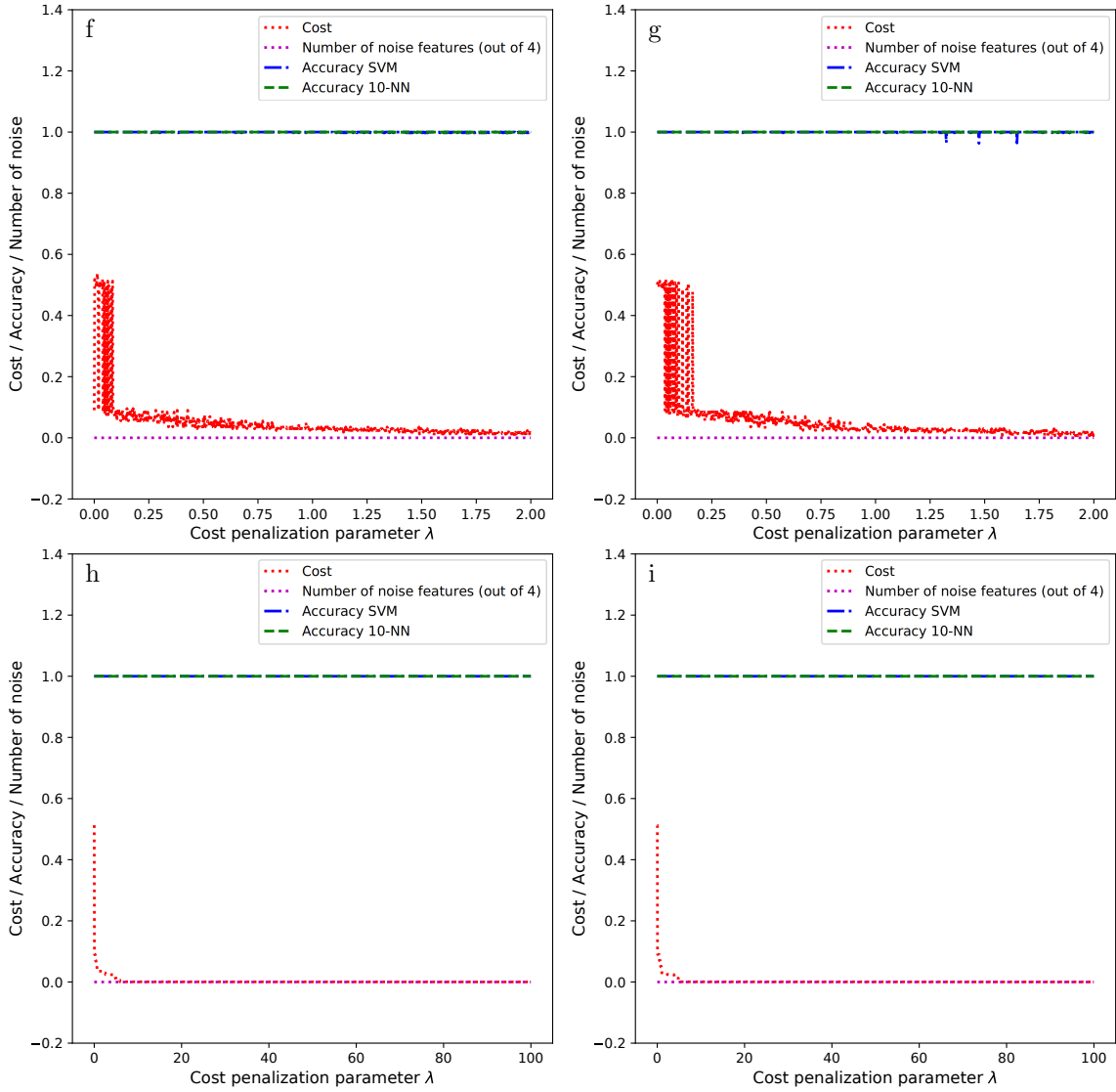


Figure 3: Same as Figure 2 but for the RF-based methods: weighted RF using MDI (panel f) or MDA (panel g), penalized RF MDI (panel h), or MDA (panel i).

connected to the new node. In other words, a random node is duplicated. For the DMC model, for each neighbor of the duplicated node, either the edge with the duplicated node or the edge with the new node is removed with probability q_{mod} . Finally, an edge between the new and the duplicated node is added with probability q_{con} . For the DMR model, only the edges adjacent to the new node are erased with probability q_{del} , and an edge between the new and duplicate node is added with probability $q_{\text{new}}/n(t)$, where $n(t)$ denotes the number of nodes in the network at the beginning of step t . These actions are repeated until the desired number of nodes, $n_o = 1000$ here, is reached.

Using a pair of connected nodes as the seed graph, each model was used to generate 2500 simulated networks, on which the same 58 summary statistics were evaluated as before (Appendix A, Table 3). The prior on parameters were uniform $\mathcal{U}_{[0.25, 0.75]}$ distributions for each parameter. We chose these bounds to avoid unlikely graphs that were either under or over-connected. These 5000 elements formed the first reference table for determining the 15 best summary statistics. A second reference table of identical size was generated and used as a validation set using 3-fold cross-validation.

Figure 4 shows that mRMR provided the worst performance of all methods: the base classification accuracy (when $\lambda = 0$) was quite low and three noise features were included. The two methods involving joint mutual information yielded greater accuracy, which could be improved for certain values of λ with the advantage of omitting the noise features while selecting a subset with low cost. The poor performance of mRMR originated from the fact that noise components are cheap and present low redundancy with other features (in the sense of $I(X_j; X_k)$), which favors their inclusion in the set of selected features. This was not the case for the JMI and JMIM methods as the conditional MIs $I(X_j; X_k | Y)$ counterbalance with $I(X_k; X_j)$ and were thus better able to avoid the inclusion of irrelevant features unless they complemented the previously selected ones. This suggests that correlation between features might be beneficial [Brown et al., 2012]. Similarly, with ReliefF, we saw decent base accuracy, which could be improved for certain values of λ while avoiding the noise summaries and reducing the total cost. This was also the case for the penalized RF importance as well as the weighted RF method, even though the latter yielded noisy curves no matter the classifier (Figure 5).

The results for the use of cost-based filter selection methods for ABC network classification are encouraging. For all methods we determined a penalization parameter value that highly decreases the total summary evaluation cost while only slightly decreasing the classification accuracy in the worst case scenario. The alternatives based on random forests provided the most reliable results for these two examples. Moreover, the use of JMI seemed preferable to mRMR as the latter failed on the more complex second example.

4 Simulation studies: utility of smaller networks

Cost-based filter selection methods are relevant to determine a set of inexpensive but informative summary statistics. However, there is a setting where the approach might be difficult to apply, specifically when the cost of obtaining the first reference table for training is high. We reduced the simulation cost of this table by reducing the number of nodes in the simulated networks. We generated networks with n_s nodes instead of n_o nodes to obtain this first reference table, and we applied the presented not cost-based filter selection methods to the table. To study the impact of employing smaller networks, we investigated two aspects: (i) the ability of the methods to select similar features when generating networks with n_s or n_o nodes; and (ii) the relevance of the selected features obtained with n_s nodes to classify networks with n_o nodes. This second aspect is important since in practice we are interested in classifying a network with n_o nodes. Note that we did not consider the cost-based versions because they present large variability in the selected summaries based on the value of λ , which made it difficult to study aspects (i) and (ii) described above. We focused on the same two classification problems presented in Section 3.

4.1 Barabási–Albert model

For classification networks from the BA models, the simulation setting was unchanged from Section 3.1 except for the size of the networks used to generate the first reference table, which was generated using networks with $n_s = 100$ nodes and then compared to the case where $n_o = 1000$.

We evaluated the ability of the selection methods to choose the same features in the two cases. To do so, we plotted the evolution of the number of common features in their selected summary subsets as a function of their size. This led to the step functions displayed in Figure 6. We represent

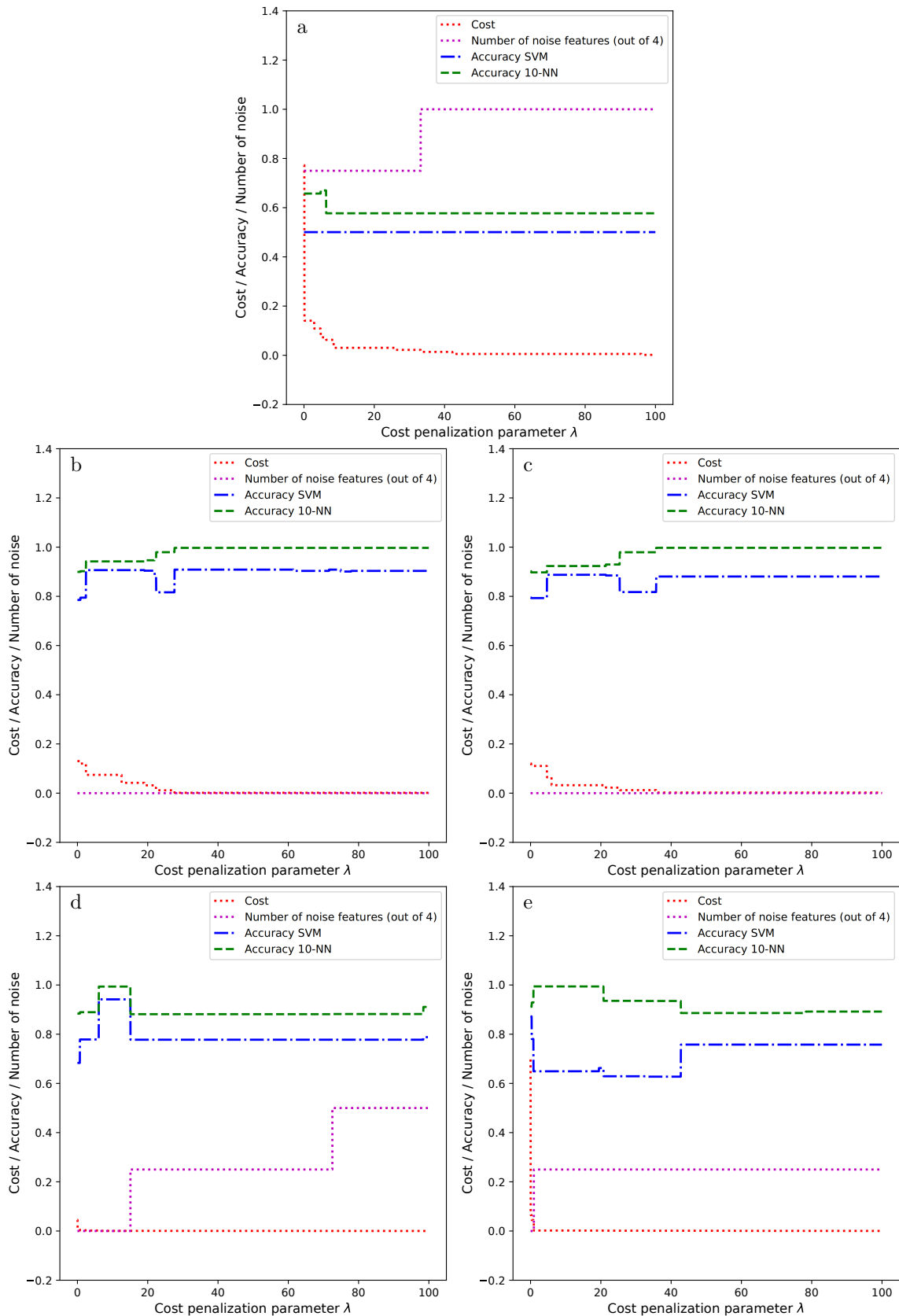


Figure 4: Evolution plots, as a function of the penalization parameter value λ , of the accuracy of the SVM and 10-NN classifiers, total cost, and proportion of noise in the summary subsets determined by the mRMR (panel a), JMI (panel b), JMIM (panel c), and ReliefF-based algorithms (panel d for the classic version and panel e for the version using RF proximity matrix). These graphs relate to the DMC versus DMR model selection problem. 15 summaries are selected out of 58.

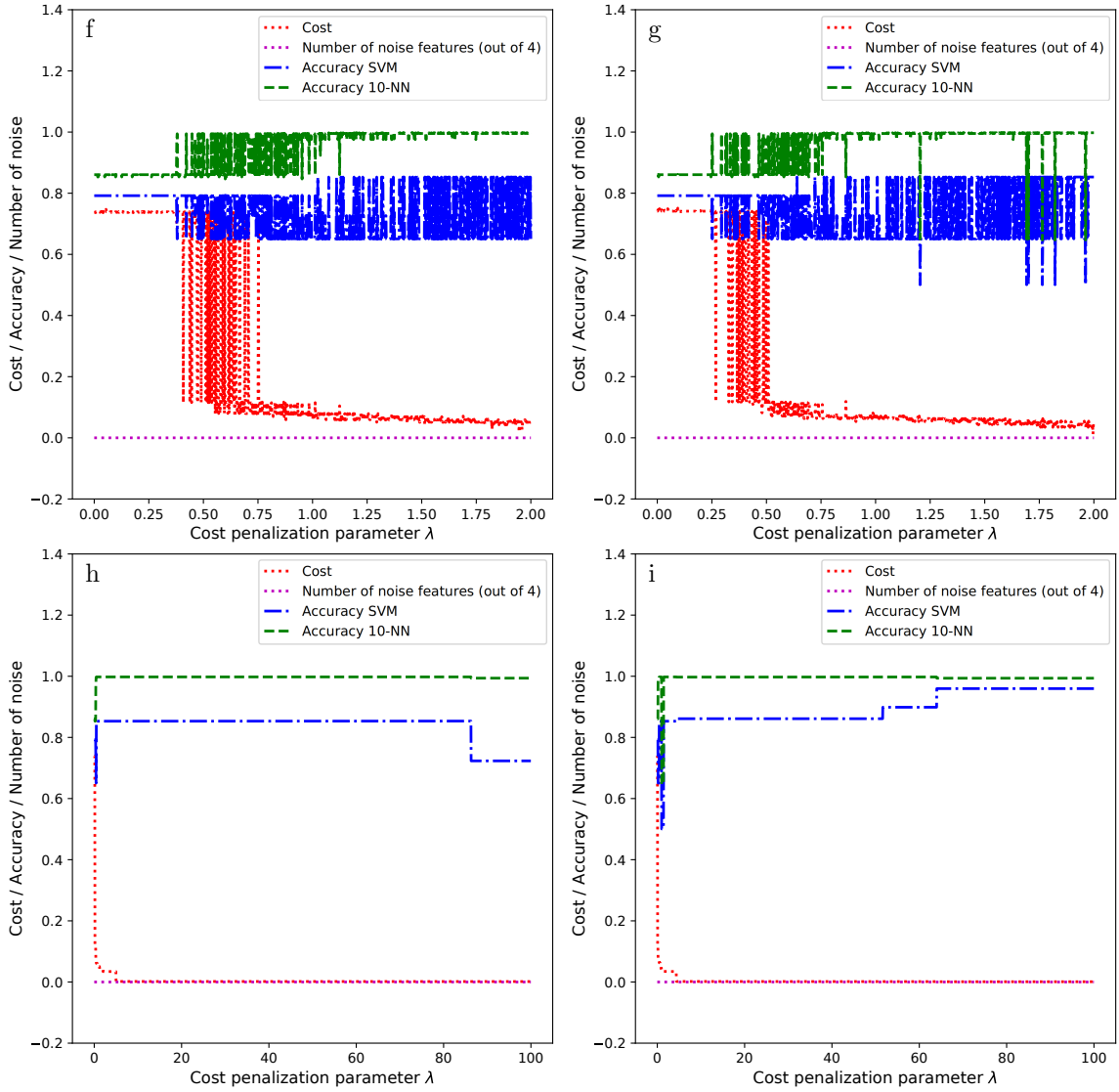


Figure 5: Same as Figure 4 but for the RF-based methods: weighted RF using MDI (panel f) or MDA (panel g), penalized RF MDI (panel h), or MDA (panel i).

the best case scenario (in black), where the use of small and large networks led to the same features being chosen for all subset sizes. For interpretation, the closer a curve is to the black curve, the better. We observed that the two ReliefF curves were very far from the optimal curve, highlighting their poor performance to select identical features. The methods based on mutual information and random forest importance, in contrast, were very close to the best case scenario.

To accurately quantify the proximity between these curves and the optimal curve, we computed the area under the curve (AUC) relative to the optimal area, using intervals ranging from 1 to $\nu \in \{5, 10, 15, 20, \dots, 45, 50\}$, and reported the average quantities and standard deviation obtained on 50 replicate analyses in Table 1. Note that this accuracy measure has the advantage of keeping track of the whole path of common selected features rather than simply averaging the number of common features for a given subset size.

Intuitively, when the subset size increased, the relative AUC moved closer to 100%, as the probability of selecting common features increased. Table 1 supports what was observed in Figure 6. The ReliefF approaches struggled to select identical features. For example, when tracking up to 25 features, the relative AUCs were 33% and 39.7%, whereas the mRMR quickly reached a value of 81.5%. The standard deviations were also considerably higher than for all other strategies. The discrepancies observed for ReliefF result from its weight update expression (Algorithm 2). Indeed, the ReliefF method is directly impacted by the distances between data with identical labels (hits) and data with different labels (misses) when projected onto each feature dimension. Even though we standardized each summary statistic, compared to networks with n_o nodes, the use of smaller networks led to different ranges of distances between data, both for identical and especially for different labels. Thus, even in a situation where classes are completely separated, the distances between data would still impact the feature weights differently when using small or large networks, and ReliefF is thus likely to provide different rankings. All the other methods showed much better performance. Their relative AUCs were high with low standard deviations for large subset sizes. For small subset sizes (5 and 10), the RF importance-based methods did not perform as well as the MI-based ones. This difference is likely explained by the presence of a large number of relevant correlated summaries, for example, those summaries based on the degree distribution. Indeed, when the same information was carried by multiple features, the RF would *share* their overall relevance among these features, and the ordering within a block of correlated features would be highly variable due to the randomness in the RF classifier [Gregorutti et al., 2017]. Unlike JMI and JMIM, which can cope with correlated features, the presence of correlated features negatively impacted the final rankings obtained with the RF when using small and large networks. Nonetheless, as described below, we found that it does not have much impact on the classification accuracy.

Method \ Set size	5	10	15	20	25	30	35	40	45	50
mRMR	54.4 (15)	70.6 (8.1)	75.6 (5.7)	79.4 (4.3)	81.5 (3.5)	82.6 (3.3)	83.8 (3.1)	85.3 (2.9)	86.8 (2.5)	88.9 (2)
JMI	48.8 (12.8)	65.1 (7)	70.7 (5.5)	77.1 (4.4)	80.1 (3.6)	81.5 (2.7)	83.1 (2.1)	85.4 (1.7)	87.8 (1.4)	90 (1.2)
JMIM	48.9 (15.5)	54.3 (9.3)	61.2 (8.3)	67.4 (7.2)	71.8 (5.5)	73.9 (4.2)	76.6 (3.4)	79.4 (3)	83 (2.4)	86 (2)
ReliefF classic	16.4 (16.6)	19.9 (14.4)	23.3 (14.7)	27.9 (14.9)	33 (14.6)	38.7 (13.1)	44.9 (11.5)	51.5 (9.8)	58.2 (8.2)	64.8 (6.8)
ReliefF RF prox.	28.4 (22.1)	29.3 (18.2)	31.5 (15.7)	34.6 (14.9)	39.7 (13.8)	45.2 (12.2)	50.8 (10.8)	56.6 (9.3)	62.6 (7.8)	68.5 (6.4)
RF MDI	27.5 (18.7)	44.8 (11.1)	59.1 (6.8)	69.7 (4.2)	74.3 (3.1)	77.2 (2.6)	80.5 (2.1)	83.6 (1.5)	85.8 (1.3)	87.5 (1.1)
RF MDA	25.5 (16.2)	46.3 (10.6)	61.2 (6.6)	71 (4)	75.1 (2.8)	77.8 (2.2)	81 (1.8)	84 (1.4)	86.1 (1.1)	87.7 (1)

Table 1: Relative areas (in percentage) under the evolution of the common selected features between networks with $n_s = 100$ nodes or $n_s = n_o = 1000$ for the classification of the four BA models. Displayed values are the average areas over 50 replicates obtained on different training tables of size 5000, and the corresponding standard deviations are in parentheses.

Even though a filter method is able to choose common features, we must ensure that the classification accuracy is similar when trying to classify networks with n_o nodes. Indeed, our objective was the classification of networks with n_o nodes, the number of nodes in the observed network. For this purpose, we used the feature subsets selected when $n_s = 100$ and $n_o = 1000$ to generate a reference table of size $N = 5000$ obtained with networks of $n_o = 1000$ nodes. On this table, using

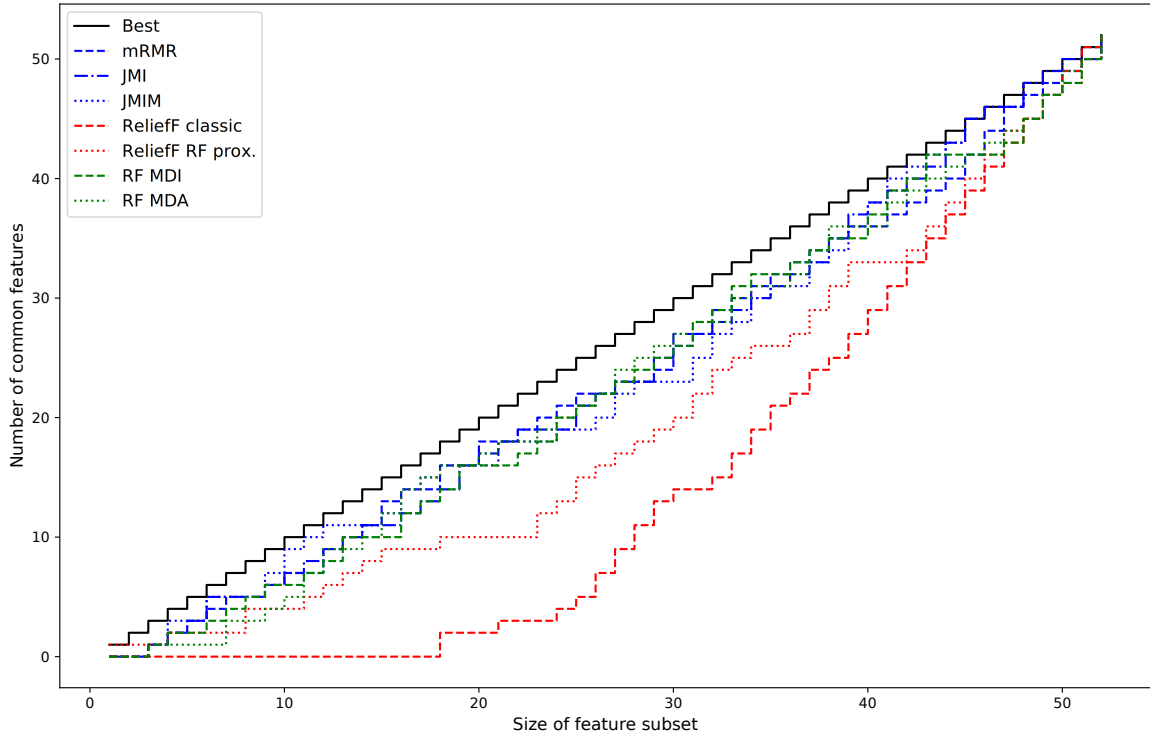


Figure 6: Evolution of the common number of selected features for the different methods when using networks with $n_s = 100$ and $n_s = n_o = 1000$ nodes. The black curve corresponds to the best scenario, i.e., when a selection method always chooses the same features for every subset size.

3-fold cross-validation, we assessed the classification accuracy of the SVM and 10-NN classifiers. Because our goal was to obtain the same accuracy with large and small networks, we computed the decrease in accuracy when using networks with $n_s = 100$ nodes rather than $n_o = 1000$ nodes for summary selection. In other words, when classifying networks with $n_o = 1000$ nodes, we computed the difference in accuracy obtained when the summary selection was performed on networks with $n_o = 1000$ nodes or $n_s = 100$ nodes: $\text{Accuracy}(n_o = 1000) - \text{Accuracy}(n_s = 100)$. Figure 7 reports the corresponding boxplots resulting from replicating the analysis 50 times. Because the ReliefF variants showed a very large decrease in classification accuracy, we omitted them from our representations. With this decrease in accuracy, a boxplot centered at zero means that the subset of summaries determined with small graphs is able to provide the same classification accuracy as those from the larger graphs. A boxplot above zero was expected because using the same network size for feature selection and classification should provide the highest accuracy. A boxplot below zero would be surprising and would suggest already poor predictive performance when using the larger number of nodes $n_o = 1000$ for selection and prediction. Finally, when the subset size increases, given the observed growth of the relative AUC (Table 1), we expected the boxplot interquartile ranges to decrease.

The decrease in accuracy with the 10-NN classifier was very low. The median was close to zero for all methods when selecting more than 10 summaries. However, the SVM showed mixed performance, with many more negative differences. Only selecting summaries with RF importance displayed almost no decrease in accuracy with boxplots centered at zero or slightly above it, no matter the feature subset size. All MI-based strategies presented a large positive or negative difference at some point, with first or third quartiles reaching $\pm 30\%$. Nonetheless, the performance of JMI was very satisfying when selecting 35 features (out of 52) or more, as was that of mRMR when selecting between 20 and 45 features. Regarding JMIM, it displayed unexpected behavior no matter the number of retained features. This suggests an already poor prediction quality from SVM when using the largest number of nodes, as observed in Section 3, Figure 4.

Finally, to understand the impact of n_s , we performed the same analysis when increasing the number of nodes from $n_s = 100$ to $n_s = 500$ (see Appendix B, Table 4 and Figure 9). Using a larger value for n_s did not change our previous conclusions, though it slightly improved most results, as expected. In Table 4, we observed that the ReliefF strategies remained unable to select the same features when using smaller or larger networks. For the MI and RF-based methods, we noticed an

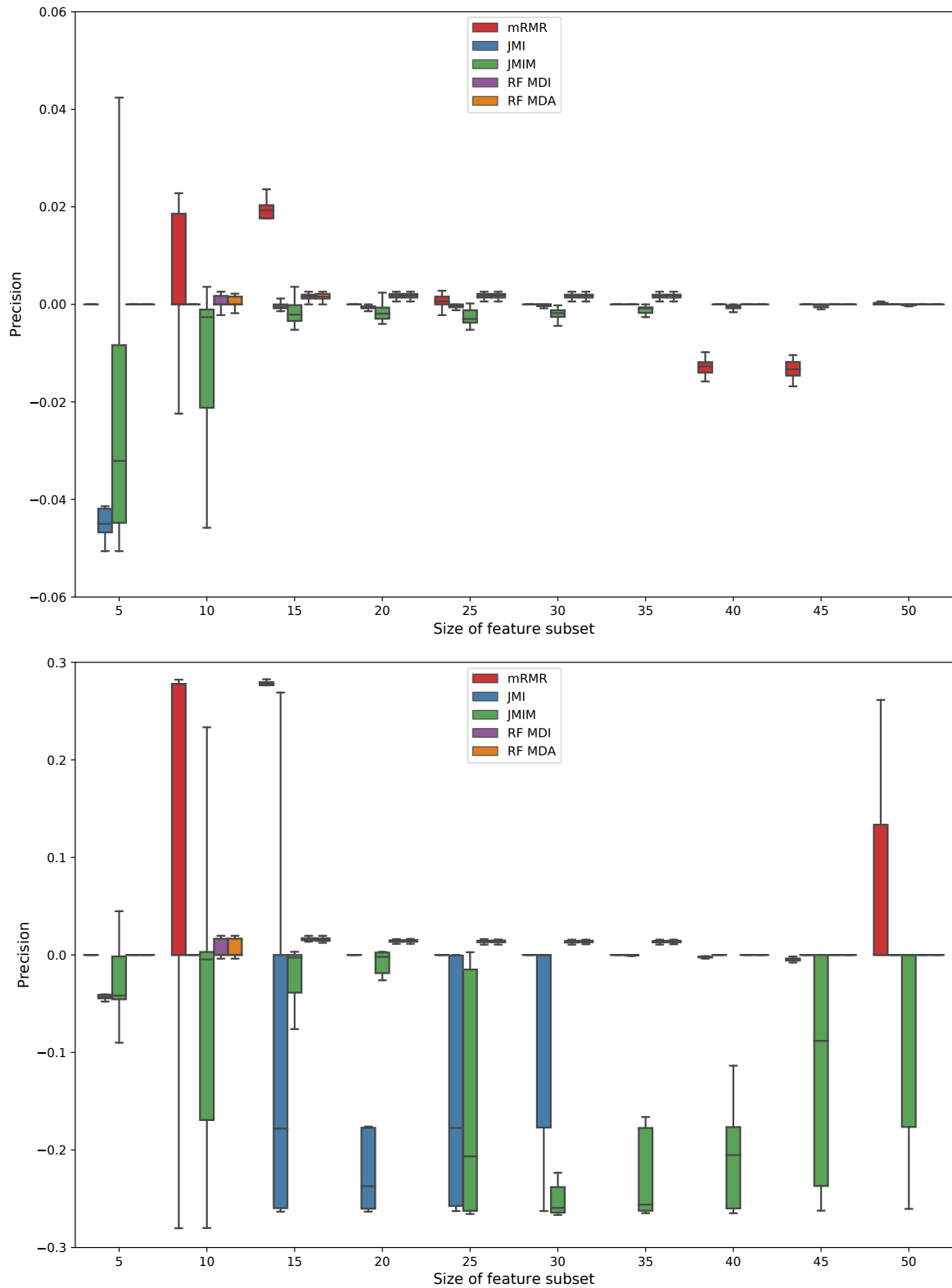


Figure 7: Boxplots of precision, here defined as the decrease in classification accuracy for networks with $n_o = 1000$ nodes when using networks with $n_s = 100$ nodes (rather than n_o nodes) for feature selection. The top and bottom graphs respectively refer to the use of a 10-NN and SVM classifiers. These graphs relate to selection of the four BA models in 50 replicate analyses.

improvement in terms of average relative AUC. This behavior was expected, because for a summary statistic that evolves as a monotonic function, its value will get closer to the observed setting as n_s increases. This improvement positively impacted the decrease in classification accuracy (Figure 9), where we observed tighter boxplot bounds and a median closer to zero for almost all methods.

4.2 Models for protein-protein interaction networks

We similarly considered the classification problem involving DMC and DMR models to analyze the quality of selected subsets with a reduced number of nodes $n_s = 100$ compared to $n_o = 1000$. With the exception of these different numbers of nodes, the simulation details were unchanged from Section 3.2. Similar to the previous section, we computed in Table 2 the relative AUCs that represent the evolution of the number of features commonly selected when $n_s = 100$ and $n_o = 1000$.

We observed that the general behavior of the methods were relatively unchanged. The ReliefF-based strategies showed poor ability to select common features. For example, when tracking up to 25 features, the relative AUCs were 32.1% and 30.3% for the ReliefF approaches, compared to 90.4% and 84.3% for mRMR and RF MDI. The standard deviations of the ReliefF were also very high, as were those for JMIM. This is again explained by the fact that the weight update expression of ReliefF is directly influenced by the range of distances between data, and using 100 nodes instead of 1000 nodes can lead to large differences in measured distance. This has less impact on the MI and RF-based methods, since the first is based on probabilities, and the second is insensitive to scale changes of the features as only the order of their values is important. For small subsets, relative AUCs of MI and RF-based strategies were higher compared to the previous example (Table 1), especially when using the RF importances. Using the MDI led to values reaching 96% and 89.8% for subset sizes of 5 and 10. This improvement is probably due to the smaller number of relevant features available to discriminate between the DMC and DMR models. In addition to having one of the largest standard deviations, the JMIM also strikingly provided the worst average relative areas after ReliefF.

Method \ Set size	5	10	15	20	25	30	35	40	45	50
mRMR	76.4 (9.1)	77.6 (5.6)	83.1 (4.2)	87.2 (3.4)	90.4 (2.2)	89.5 (1.9)	88 (1.9)	87.1 (1.5)	87.4 (1.2)	89 (1.1)
JMI	68.7 (9.1)	71.8 (6.2)	77.2 (6.1)	77.3 (5.7)	76.5 (5.6)	78.9 (5.7)	79.5 (5.4)	81.9 (5)	83.6 (4.2)	85.6 (3.4)
JMIM	55.7 (12.8)	61.4 (12)	67.9 (13.6)	67.4 (14.7)	67.8 (15.8)	68.4 (16.7)	70 (17.2)	73 (16.4)	75.8 (14.7)	78.6 (12.7)
ReliefF classic	13.6 (17)	18.3 (14.1)	23 (13.2)	27.4 (11.8)	32.1 (11.2)	37.6 (10.8)	43.2 (10.1)	48.7 (9.1)	54.2 (8.1)	59.8 (7.1)
ReliefF RF prox.	9.1 (17.2)	14.4 (15.7)	19.1 (14.5)	24.7 (14.8)	30.3 (14.6)	36.2 (14.1)	42.2 (13.1)	48.2 (11.8)	54.1 (10.5)	59.8 (9)
RF MDI	96 (4.4)	89.8 (2.5)	87.1 (2.3)	86.4 (1.7)	84.3 (1.7)	84.5 (1.5)	85.4 (1.4)	86.7 (1.2)	88.1 (1)	89.7 (0.9)
RF MDA	74.1 (5.6)	70.7 (5)	76.6 (3)	79.7 (2)	80.2 (1.7)	81.5 (1.6)	83.3 (1.4)	84.8 (1.2)	86.5 (0.9)	88.7 (0.8)

Table 2: Relative areas (in percentage) under the evolution of the common selected features between networks with $n_s = 100$ nodes or $n_s = n_o = 1000$ for the DMC versus DMR model classification problem. Displayed values are the average areas over 50 replicates obtained on different training tables of size 5000, and the corresponding standard deviations are in parentheses.

As in the previous section, we computed the difference in classification accuracy when using the larger and smaller numbers of nodes (Figure 8). The two classifiers, 10-NN and SVM showed similar behavior, even though the latter presented slightly larger interquartile ranges. When selecting 15 summaries or more, the MI-based methods provided the best results, with narrow boxplots centered at zero (except for the JMIM for a subset size equal to 50). The RF-based methods illustrate the negative impact of using smaller networks for selection, as they degraded the classifier performance with median values in the vicinity of 30%. However, the decrease in accuracy when using the MDA returned to zero when selecting 35 features or more (out of 58). For the RF-based methods, we noticed a sudden change in the boxplot location in the positive range, which then returned to zero for a larger subset size. This suggests that for a given number of selected features, those relevant for classification of networks with $n_o = 1000$ nodes were first identified when using networks with the same number of nodes; only inclusion of a larger number of summaries (i.e., for a larger subset size)

allowed the use of smaller networks to identify these relevant summaries, and therefore centered the boxplots back toward zero. We performed the same analysis when $n_s = 500$ (see Appendix C, Table 5 and Figure 10), and observed that these atypical behaviors in the boxplot location were mostly erased, which was quite encouraging but also highlights the danger of using a value for n_s that is too low.

Concerning the second question of this paper, of the two examples studied, it was not obvious that summaries selected with smaller graphs could be used to classify larger networks reliably. The ReliefF methods were clearly not designed for such a purpose as their criterion was too severely affected by the difference in the range of distances between data, leading to different summary statistic rankings as observed in Tables 1 and 2. The most promising filter selection methods able to preserve the classifier accuracy were the mRMR, the JMI, and the RF importance based on MDA, as they showed the smallest changes in accuracy. However, when crossed with the raw classification accuracy, the mRMR did not seem very consistent between examples (see Figure 4, with $\lambda = 0$, panel a), so it might be avoided. Nonetheless, the behavior of JMI and the RF MDA could still be unpredictable when eliminating too many summaries at once. For these two methods, eliminating up to one-third of the basic summaries appears to be a safe choice, at least with the two examples presented here. Naturally, the closer the n_s value gets to n_o the better, at the price of a higher computational cost required to perform selection.

5 Discussion

Performing summary statistic selection is critical for most ABC inferential methods. This is especially important when studying mechanistic network models with summary statistics that are computationally intensive to evaluate. We showed that cost-based feature selection algorithms can be used advantageously to greatly reduce the evaluation cost of selected summaries compared to not cost-based versions without much impact on the classification accuracy. Even though we focused on filter selection methods that provide a ranking of the features (mostly in a forward fashion), more complicated subset exploration strategies can be employed that are not limited to the filter category. The proposal of Zhang et al. [2019], i.e., a cost-based wrapper algorithm with subset exploration based on artificial bee colony, could be an interesting method to explore. Moreover, the cost-based literature is currently sparse and transposing recent selection algorithms, such as additional versions of ReliefF methods, to this framework would be highly beneficial [Urbanowicz et al., 2018a].

We also investigated the relevance of summary statistic selection using networks that have fewer nodes than the observed network. We found that eliminating too many summaries at once can be harmful since relevant summaries selected using small networks are less likely to coincide with the summaries obtained using large networks with n_o nodes. Network size directly impacts the selected features: the more closely the size of the network used for feature selection matches the size of the observed network, the better the results. Nonetheless, using JMI or RF importance measures yields the most reliable summary subsets provided that the number of eliminated summaries is small. Given this finding, an interesting extension of our approach would be to consider an iterative selection algorithm based on small networks, where only a small number of features are discarded at each step until the desired number of selected features is reached.

We recently investigated two approaches for ABC parameter inference that could be adapted for summary statistic selection [Raynal et al., 2020]. The first approach consists of replacing the values of summary statistics computed on simulated networks with n_o nodes with extrapolated summary statistics computed on smaller networks with $n_s < n_o$ nodes. As expected, and as observed here, results improved as n_s gets closer to n_o . An interesting alternative to the use of smaller networks for summary statistics selection would thus be to use summary statistics extrapolated to n_o nodes for the most computationally demanding summaries. While such an approach would be impacted by the extrapolation quality at n_o , the benefit is that summary statistic selection would make use of (extrapolated) summaries for networks with n_o nodes, the same as the observed graph. The other approach, investigated in Raynal et al. [2020], is the use of extrapolated sample-based summary statistics, where certain summaries are computed on subgraphs of networks with n_o nodes. When omitting the extrapolation part, replacing the summaries with high cost by sample-based versions could be an alternative approach to scalable selection.

In this paper, we evaluated the accuracy of SVM and k -NN classifiers and showed that for cost-based filter selection methods, the penalization parameter (λ) can be tuned such that the computational cost of generating summary statistics is reduced without compromising their predictive performance. Since the selected summaries depend on the specific classifier, it is not obvious whether

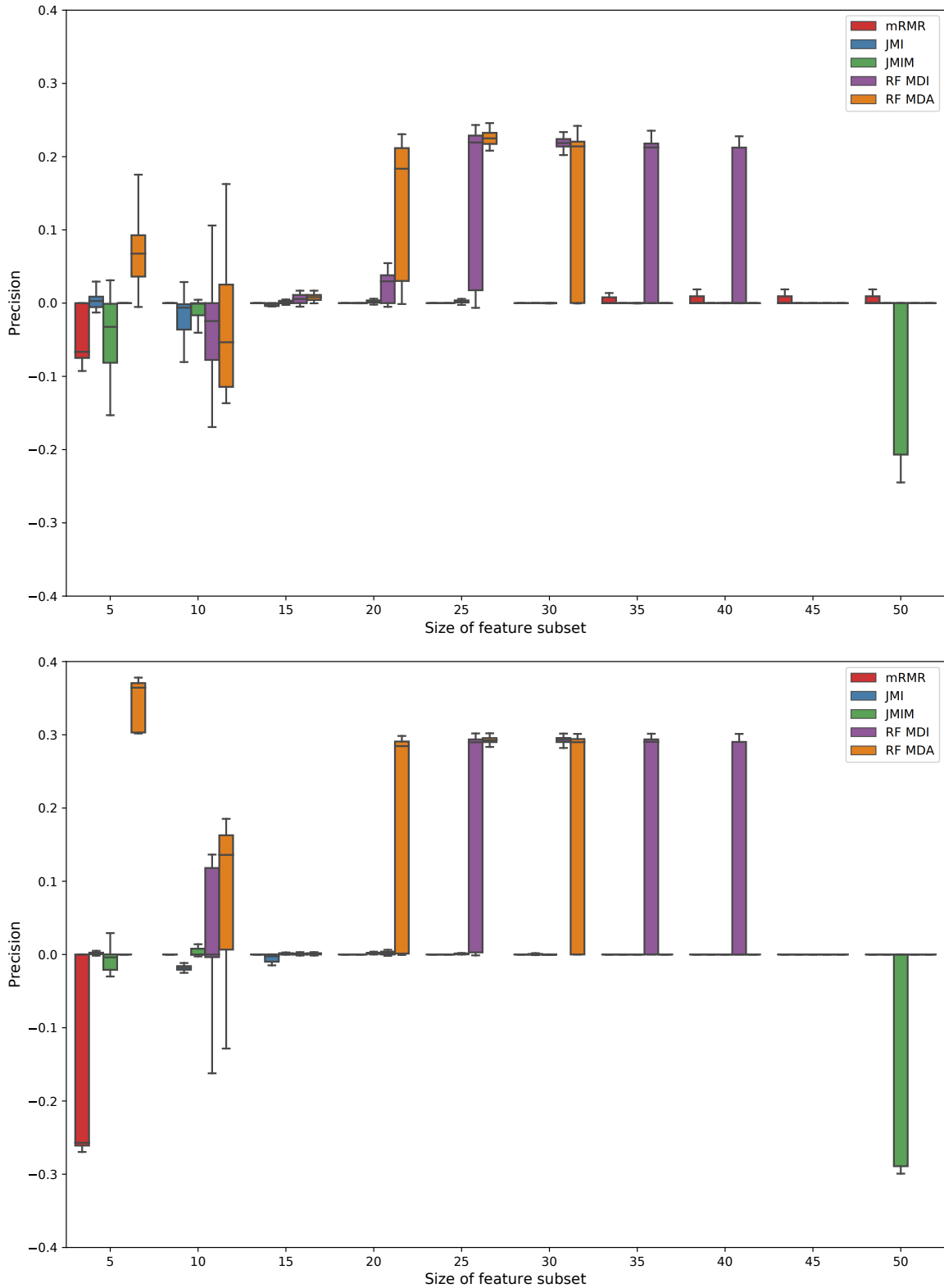


Figure 8: Boxplots of precision, here defined as the decrease in classification accuracy for networks with $n_o = 1000$ nodes when using networks with $n_s = 100$ nodes (rather than n_o nodes) for feature selection. The top and bottom graphs refer to the use of a 10-NN and SVM classifiers, respectively. These graphs relate to the DMC versus DMR model selection problem in 50 replicate analyses.

summaries selected by one classifier would also be selected by another classifier. Nonetheless, because classic filter selection methods are classifier independent, the selected summaries can, in principle, be used with any classifier or with more computationally demanding ABC methods.

Code availability

Python codes are available at both github.com/LouisRaynal/cost_based_selection or github.com/onnela-lab/net_summary_selection.

Acknowledgments

We would like to thank Antonietta Mira for some useful discussions about summary statistic selection, Hali Hambridge and Jonathan Larson for their useful comments and corrections on the manuscript, as well as Amanda King for proofreading the early version of this paper. This project was supported by the U.S. National Institutes of Health award R01AI138901.

References

- A. L. Barabási and R. Albert. Emergence of scaling in random networks. *science*, 286(5439):509–512, 1999. [3](#), [9](#)
- M. Bannasar, Y. Hicks, and R. Setchi. Feature selection using Joint Mutual Information Maximisation. *Expert Systems With Applications*, 42:8520–8532, 2015. [6](#)
- G. Biau and E. Scornet. A random forest guided tour. *TEST*, 25(2):197–227, 2016. [8](#)
- G. Biau, F. Cérou, and A. Guyader. New insights into approximate Bayesian computation. *Annales de l'Institut Henri Poincaré B, Probability and Statistics*, 51(1):376–403, 2015. [9](#)
- M. G. B. Blum. Choosing the summary statistics and the acceptance rate in approximate Bayesian computation. In Y. Lechevallier and G. Saporta, editors, *Proceedings of COMPSTAT'2010.*, pages 47–56. Physica-Verlag HD, 2010. [2](#)
- M. G. B. Blum, M. Nunes, D. Prangle, and S. A. Sisson. A comparative review of dimension reduction methods in approximate Bayesian computation. *Statistical Science*, 28(2):189–208, 2013. [3](#)
- V. Bolón-Canedo, I. Porto-Díaz, N. Sánchez-Marroño, and A. Alonso-Betanzos. A framework for cost-based feature selection. *Pattern Recognition*, 47:2481–2489, 2014a. [4](#)
- V. Bolón-Canedo, B. Remeseiro, N. Sánchez-Marroño, and A. Alonso-Betanzos. mC-ReliefF: An Extension of ReliefF for Cost-Based Feature Selection. In *6th International Conference on Agents and Artificial Intelligence (ICAART)*, volume 1, 2014b. [4](#), [6](#), [7](#), [8](#)
- L. Breiman. Random forests. *Machine Learning*, 45:5–32, 2001. [2](#), [4](#), [5](#), [8](#)
- L. Breiman, J. Friedman, C. J. Stone, and R. A. Olshen. *Classification and Regression Trees*. The Wadsworth and Brooks-Cole statistics-probability series. Taylor & Francis, 1984. [8](#)
- G. Brown, A. Pocock, M.-J. Zhao, and M. Luján. Conditional Likelihood Maximisation: A Unifying Framework for Information Theoretic Feature Selection. *Journal of Machine Learning Research*, 13:27–66, 2012. [6](#), [13](#)
- S. Chen, A. Mira, and J.-P. Onnela. Flexible model selection for mechanistic network models. *Journal of Complex Networks*, cnz024, 2019. [2](#), [3](#)
- F. D. Collin, G. Durif, L. Raynal, E. Lombaert, M. Gautier, R. Vitalis, J.-M. Marin, and A. Estoup. Extending Approximate Bayesian Computation with Supervised Machine Learning to infer demographic history from genetic polymorphisms using DIYABC Random Forest. *Submitted to Molecular Ecology Resources*, jul 2020. doi: 10.22541/au.159480722.26357192. URL <https://doi.org/10.22541%2Fau.159480722.26357192>. [2](#)
- P. Del Moral, A. Doucet, and A. Jasra. An adaptive sequential Monte Carlo method for approximate Bayesian computation. *Statistics and Computing*, 22(5):1009–1020, 2012. [2](#)

- R. Dutta, A. Mira, and J.-P. Onnela. Bayesian inference of spreading processes on networks. *Proceedings of the Royal Society A: Mathematical, Physical and Engineering Sciences*, 474(2215):20180129, 2018. [2](#)
- A. Estoup, E. Lombaert, J.-M. Marin, C. P. Robert, T. Guillemaud, P. Pudlo, and J.-M. Cornuet. Estimation of demo-genetic model probabilities with approximate Bayesian computation using linear discriminant analysis on summary statistics. *Molecular Ecology Resources*, 12(5):846–855, 2012. [3](#)
- Y. Fan, S. R. Meikle, G. I. Angelis, and A. Sitek. Abc in nuclear imaging. In S. A. Sisson, Y. Fan, and M. A. Beaumont, editors, *Handbook of Approximate Bayesian Computation*. Chapman and Hall/CRC, 2018. 623-647. [2](#)
- M. Fasiolo and S. N. Wood. Abc in ecological modelling. In S. A. Sisson, Y. Fan, and M. A. Beaumont, editors, *Handbook of Approximate Bayesian Computation*. Chapman and Hall/CRC, 2018. 597-622. [2](#)
- P. Fearnhead and D. Prangle. Constructing summary statistics for approximate Bayesian computation: semi-automatic approximate Bayesian computation. *Journal of the Royal Statistical Society. B (Statistical Methodology)*, 74(3):419–474, 2012. [2](#)
- S. Fortunato. Community detection in graphs. *Physics reports*, 486(3-5):75–174, 2010. [2](#)
- B. Gregorutti, B. Michel, and P. Saint-Pierre. Correlation and variable importance in random forests. *Statistics and Computing*, 27(3):659–678, 2017. [16](#)
- A. A. Hagberg, D. A. Schult, and P. J. Swart. Exploring network structure, dynamics, and function using NetworkX. In *Proceedings of the 7th Python in Science Conference (SciPy2008)*, page 11–15, Pasadena, CA USA, Aug 2008. Gäel Varoquaux, Travis Vaught, and Jarrod Millman (Eds). [9](#), [26](#)
- P. B. Holden, N. R. Edwards, J. Hensman, and R. D. Wilkinson. Abc for climate: dealing with expensive simulators. In S. Sisson, Y. Fan, and M. A. Beaumont, editors, *Handbook of Approximate Bayesian Computation*. Chapman and Hall/CRC, 2018. 569-595. [2](#)
- F. Hormozdiari, P. Berenbrink, N. Pržulj, and S. C. Sahinalp. Not All Scale-Free Networks Are Born Equal: The Role of the Seed Graph in PPI Network Evolution. *PLOS Computational Biology*, 3:1–12, 2007. [9](#)
- R. Jagdhuber, M. Lang, A. Stenzl, J. Neuhaus, and J. Rahnenführer. Cost-Constrained feature selection in binary classification: adaptations for greedy forward selection and genetic algorithms. *BMC Bioinformatics*, 21:26, 2020. [4](#)
- A. Jović, K. Brkić, and N. Bogunović. A review of feature selection methods with applications. In *2015 38th International Convention on Information and Communication Technology, Electronics and Microelectronics (MIPRO)*, pages 1200–1205, 2015. [3](#)
- K. Kira and L. A. Rendell. The Feature Selection Problem: Traditional Methods and a New Algorithm. *AAAI*, 2:129–134, 1992. [5](#), [7](#)
- I. Kononenko. Estimating attributes: Analysis and extensions of relief. In F. Bergadano and L. De Raedt, editors, *Machine Learning: ECML-94*, pages 171–182, Berlin, Heidelberg, 1994. Springer Berlin Heidelberg. [4](#), [7](#)
- J. Liepe and M. P. H. Stumpf. Abc in systems biology. In S. Sisson, Y. Fan, and M. A. Beaumont, editors, *Handbook of Approximate Bayesian Computation*. Chapman and Hall/CRC, 2018. 513-539. [2](#)
- D. Lusher, J. Koskinen, and G. Robins. *Exponential random graph models for social networks: Theory, methods, and applications*. Cambridge University Press, 2013. [2](#)
- M. Newman. *Networks: an introduction*. Oxford university press, 2010. [2](#)
- M. A. Nunes and D. J. Balding. On optimal selection of summary statistics for approximate Bayesian computation. *Statistical Application in Genetics and Molecular Biology*, 9(1):Article 34, 2010. [2](#)
- J.-P. Onnela and A. Mira. Statistical inference and model selection for mechanistic network models. *In progress*, In progress. [2](#)

- H. Peng, F. Long, and C. Ding. Feature Selection Based on Mutual Information: Criteria of Max-Dependency, Max-Relevance, and Min-Redundancy. *IEEE Transactions on pattern analysis and machine intelligence*, 27:1226–1238, 2005. 4, 5
- D. Prangle. Adapting the ABC distance function. *Bayesian Analysis*, 12(1):289–309, 2017. 2
- D. Prangle. Summary statistics. In S. A. Sisson, Y. Fan, and M. A. Beaumont, editors, *Handbook of Approximate Bayesian Computation*. Chapman and Hall/CRC, 2018. 125-152. 2
- J. K. Pritchard, M. T. Seielstad, A. Perez-Lezaun, and M. W. Feldman. Population growth of human Y chromosomes: a study of Y chromosome microsatellites. *Molecular Biology and Evolution*, 16: 1791–1798, 1999. 2
- P. Pudlo, J.-M. Marin, A. Estoup, J.-M. Cornuet, M. Gautier, and C. P. Robert. Reliable ABC model choice via random forests. *Bioinformatics*, 32(6):859–866, 2016. 2, 3
- L. Raynal, J.-M. Marin, P. Pudlo, M. Ribatet, C. P. Robert, and A. Estoup. ABC random forests for Bayesian parameter inference. *Bioinformatics*, 35(10):1720–1728, 2019. 2
- L. Raynal, S. Chen, A. Mira, and J.-P. Onnela. Scalable Approximate Bayesian Computation for Growing Network Models via Extrapolated and Sampled Summaries. *submitted to Bayesian Analysis, ...*, 2020. 2, 20
- G. S. Rodrigues, A. R. Francis, S. A. Sisson, and M. M. Tanaka. Inference on the acquisition of multi-drug resistance in mycobacterium tuberculosis using molecular epidemiological data. In S. Sisson, Y. Fan, and M. A. Beaumont, editors, *Handbook of Approximate Bayesian Computation*. Chapman and Hall/CRC, 2018. 482-511. 2
- B. C. Ross. Mutual Information between Discrete and Continuous Data Sets. *PLOS ONE*, 9:e87357, 2014. 6
- R. Schweiger, M. Linial, and L. N. Generative probabilistic models for protein-protein interaction networks—the biclique perspective. *Bioinformatics*, 27:i142–i148, 2011. 9
- M. A. Sedki and P. Pudlo. Contribution to the discussion of Fearnhead and Prangle (2012). *Journal of the Royal Statistical Society. B (Statistical Methodology)*, 74(3):466–467, 2012. 3
- C. E. Shannon. A mathematical theory of communication. *Bell Systems Technical Journal*, 27: 379–423, 1948. 3, 5
- S. Sheehan and Y. S. Song. Deep learning for population genetic inference. *PLOS Computational Biology*, 12(3), 2016. 2
- S. Sisson, Y. Fan, and M. Tanaka. Sequential Monte Carlo without likelihoods: Errata. *Proceedings of the National Academy of Sciences, USA*, 106(39):16889, 2009. 2
- R. V. Solé, R. Pastor-Satorras, E. Smith, and T. B. Kepler. A model of large-scale proteome evolution. *Advances in Complex Systems*, 5(1):43–54, 2002. 3, 10
- V. Thouzeau, P. Menecier, P. Verdu, and F. Austerlitz. Genetic and linguistic histories in Central Asia inferred using approximate Bayesian computations. *Proceedings of the Royal Society of London B: Biological Sciences*, 284(1861), 2017. 2
- R. Tibshirani. Regression Shrinkage and Selection via the Lasso. *Journal of the Royal Statistical Society. B (Statistical Methodology)*, 58(1):267–288, 1996. 4
- V. A. Traag, P. Van Dooren, and Y. Nesterov. Narrow scope for resolution-limit-free community detection. *Physical Review E*, 84(1):016114, 2011. 2
- R. J. Urbanowicz, M. Meeker, W. La Cava, R. S. Olson, and M. J. J. Relief-Based Feature Selection: Introduction and Review. *Journal of Biomedical Informatics*, 85:189–203, 2018a. 5, 7, 20
- R. J. Urbanowicz, R. S. Olson, P. Schmitt, M. Meeker, and J. H. Moore. Benchmarking relief-based feature selection methods for bioinformatics data mining. *Journal of Biomedical Informatics*, 85: 168–188, 2018b. 7
- M. J. van der Laan, E. C. Polley, and A. E. Hubbard. Super Learner. *Statistical Applications in Genetics and Molecular Biology*, 6(1), 2007. 2, 10

- A. Vázquez, A. Flammini, A. Maritan, and A. Vespignani. Modeling of protein interaction networks. *Complexus*, 1:38–44, 2003. [3](#), [10](#)
- H. H. Yang and J. Moody. Feature selection based on joint mutual information. In *Advances in intelligent data analysis, proceedings of international ICSC symposium*, pages 22—25, 1999. [6](#)
- Y. Zhang, S. Cheng, Y. Shi, D.-W. Gong, and X. Zhao. Cost-sensitive feature selection using two-archive multi-objective artificial bee colony algorithm. *Expert Systems With Applications*, 137: 46–58, 2019. [4](#), [20](#)
- Q. Zhou, H. Zhou, and T. Li. Cost-sensitive feature selection using random forest: Selecting low-cost subsets of informative features. *Knowledge-Based Systems*, 95:1–11, 2016. [4](#), [8](#)

A Network summary statistics computed

General structure	
Number of edges	Number of connected components
Number of nodes in LCC	Number of edges in LCC
Distance/Path	
Diameter of the LCC	Average geodesic distance in LCC
Average shortest path length in LCC	Average global efficiency
Inverse global efficiency	Average local efficiency in LCC
Wiener index in LCC	
Centrality	
Average degree connectivity	Average degree connectivity in LCC
Average degree connectivity	Entropy of the DD
Maximal degree	Average degree
Median degree	Standard deviation of the DD
25% quantile of the DD	75% quantile of the DD
Node connectivity in LCC	Edge connectivity in LCC
Average betweenness centrality	Maximal betweenness centrality
Average egevector centrality	Maximal egevector centrality
Central point dominance	Estrada index
Groups of nodes	
Transitivity	Number of triangles
Average clustering coefficient	Average square clustering
Median square clustering	Std.-dev. square clustering
Number of 2-cores	Number of 3-cores
Number of 4-cores	Number of 5-cores
Number of 6-cores	Number of 2-shells
Number of 3-shells	Number of 4-shells
Number of 5-shells	Number of 6-shells
Number of 4-cliques	Number of 5-cliques
Number of 3-shortest paths	Number of 4-shortest paths
Number of 5-shortest paths	Number of 6-shortest paths
Maximal clique size	Approximate size of a large clique
Size of the minimum node dominating set	Size of the minimum edge dominating set
Simulated noise	
$\mathcal{N}(0, 1)$	$\mathcal{U}_{[0, 50]}$
$\mathcal{Ber}(0.5)$	Discrete $\mathcal{U}_{[0, 50]}$

Table 3: The 58 network summary statistics considered. All can be easily computed with the Python package `NetworkX` [Hagberg et al., Aug 2008]. LCC stands for “largest connected component” and DD stands for “degree distribution.”

B Selection with smaller networks: Barabási-Albert model classification

Method \ Set size	5	10	15	20	25	30	35	40	45	50
mRMR	68 (19.3)	77.5 (11)	80.1 (8.3)	83.3 (6.2)	84.3 (4.7)	85.8 (3.9)	87.1 (3.3)	88.2 (2.8)	89.3 (2.3)	91.1 (1.8)
JMI	40.3 (13.7)	58.2 (5.9)	71.5 (5.5)	78.3 (3.7)	83.3 (3.1)	85.6 (2.7)	87.7 (2.2)	90 (1.8)	91.9 (1.5)	93.3 (1.3)
JMIM	51.1 (17.8)	54.6 (12.5)	59.8 (10.4)	66.2 (8.5)	71.1 (7)	75.2 (5.9)	79.3 (5)	82.4 (4.5)	85.4 (3.7)	88 (3.1)
ReliefF classic	21.3 (24.7)	21.9 (21.2)	24.8 (21.4)	29.2 (21.5)	33.9 (20.6)	39.4 (18.9)	45.6 (16.6)	52.3 (14.3)	58.9 (12)	65.4 (9.9)
ReliefF RF prox.	25.9 (21.4)	30.6 (17.9)	35.2 (19)	39.6 (19)	44.5 (18)	49.4 (16.2)	55 (14.5)	60.6 (12.6)	66 (10.6)	71.4 (8.8)
RF MDI	21.7 (15.8)	41.1 (11.9)	58.2 (7.7)	72.2 (4.7)	78.7 (3.4)	81.5 (2.6)	84.6 (2)	87.7 (1.6)	89.6 (1.3)	91 (1.1)
RF MDA	26 (15.1)	45.3 (12.3)	61.8 (7.5)	74.8 (4.7)	80.2 (3.4)	82.8 (2.8)	85.6 (2.2)	88.5 (1.7)	90.2 (1.4)	91.5 (1.2)

Table 4: Relative areas (in percentage) under the evolution of the common selected features between networks with $n_s = 500$ nodes or $n_s = n_o = 1000$ for the classification of the four BA models. Displayed values are the average areas over 50 replicates obtained on different training tables of size 5000, and the corresponding standard deviations are in parentheses.

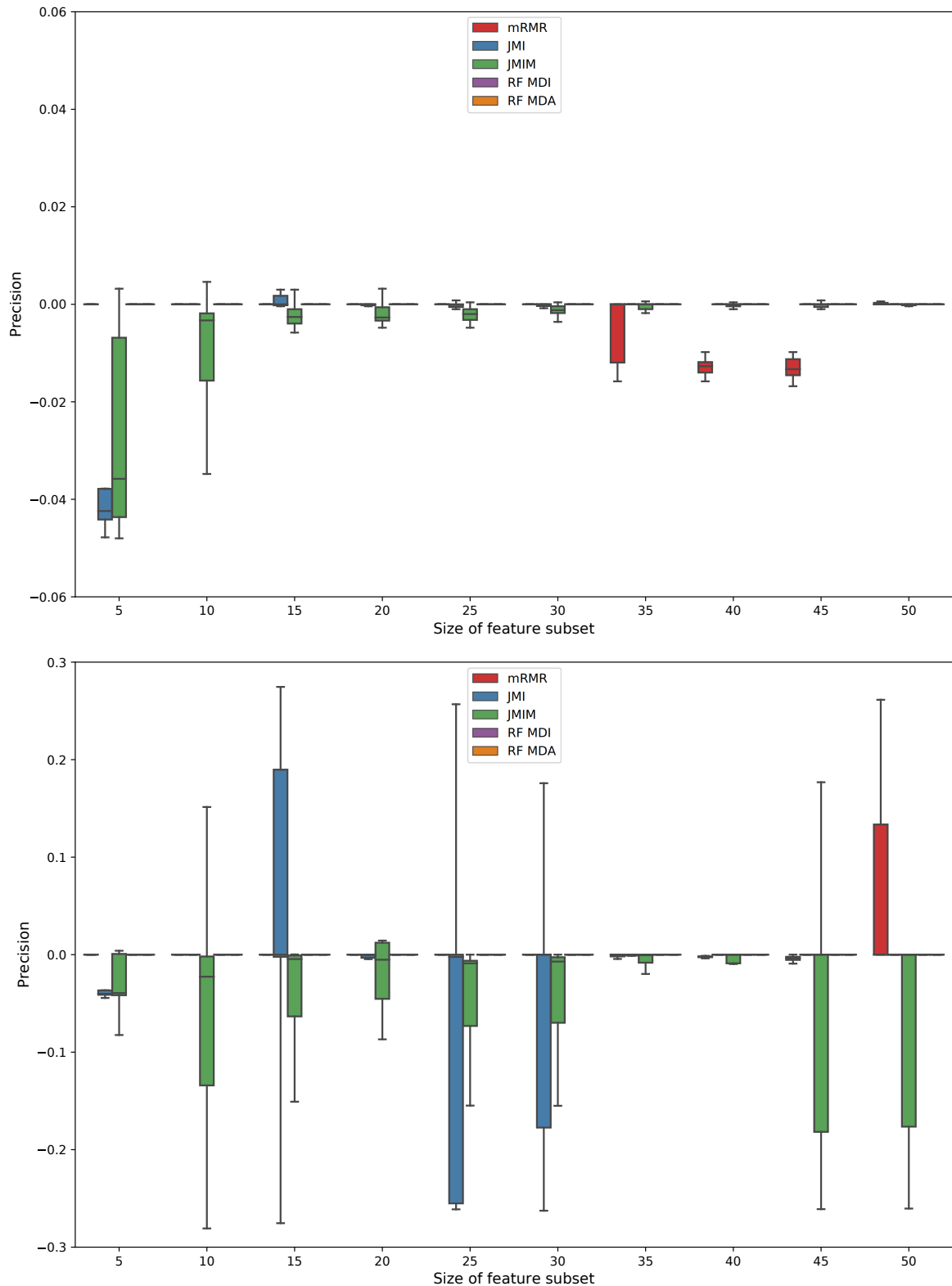


Figure 9: Boxplots of precision, here defined as the decrease in classification accuracy for networks with $n_o = 1000$ nodes when using networks with $n_s = 500$ nodes (rather than n_o nodes) for feature selection. The top and bottom graphs refer to the use of a 10-nearest neighbors and SVM classifiers, respectively. These graphs relate to selection of the four BA models in 50 replicate analyses.

C Selection with smaller networks: DMC-DMR model classification

Method \ Set size	5	10	15	20	25	30	35	40	45	50
mRMR	76.8 (10.5)	81.1 (5.9)	87.1 (4.1)	90.2 (3.4)	93 (2.1)	93.5 (1.7)	93.5 (1.5)	93 (1.3)	93.7 (1.1)	94.6 (1)
JMI	64.5 (12.4)	78.9 (9.9)	84.5 (8.7)	86.1 (6.1)	88.2 (5.6)	89.2 (5.5)	90.6 (5.2)	91.5 (5)	91.9 (4.3)	93.1 (3.6)
JMIM	50 (12.2)	57.5 (11.2)	66.7 (12.9)	69.2 (14.2)	70.6 (14.4)	72 (14.3)	73.6 (14.1)	75.7 (13.5)	78.5 (12.5)	81.3 (11.2)
ReliefF classic	12.1 (16.3)	18.7 (15.8)	23.8 (16.6)	28.7 (16.5)	33.6 (16.1)	38.6 (15.2)	43.9 (13.9)	49.2 (12.3)	54.6 (10.7)	60.2 (9.2)
ReliefF RF prox.	9.1 (17.3)	14.8 (16.4)	20.1 (15.6)	26 (15.6)	31.7 (15.2)	37.1 (14.2)	42.4 (13.1)	47.9 (11.8)	53.5 (10.2)	59.2 (8.6)
RF MDI	94.8 (5.7)	93.7 (3)	93.6 (1.9)	94.5 (1.1)	93.2 (1.3)	93.3 (1.2)	93.4 (0.9)	93.7 (0.9)	93.9 (0.7)	94.4 (0.6)
RF MDA	89.6 (6.4)	90.1 (2.9)	92.2 (2.2)	92 (1.6)	90.8 (1.6)	91.1 (1.5)	92.1 (1.1)	92.5 (0.9)	93 (0.8)	94 (0.7)

Table 5: Relative areas (in percentage) under the evolution of the common selected features between networks with $n_s = 500$ nodes or $n_s = n_o = 1000$ for the DMC versus DMR model classification problem. Displayed values are the average areas over 50 replicates obtained on different training tables of size 5000, and the corresponding standard deviations are in parentheses.

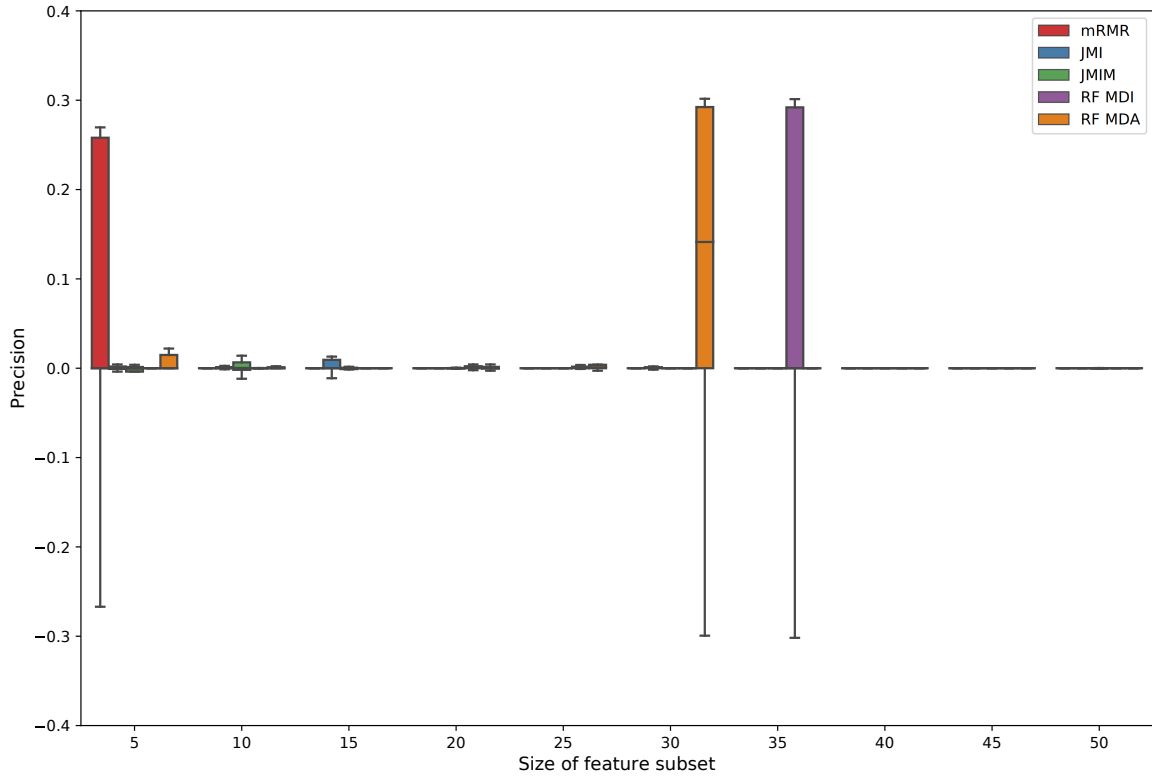
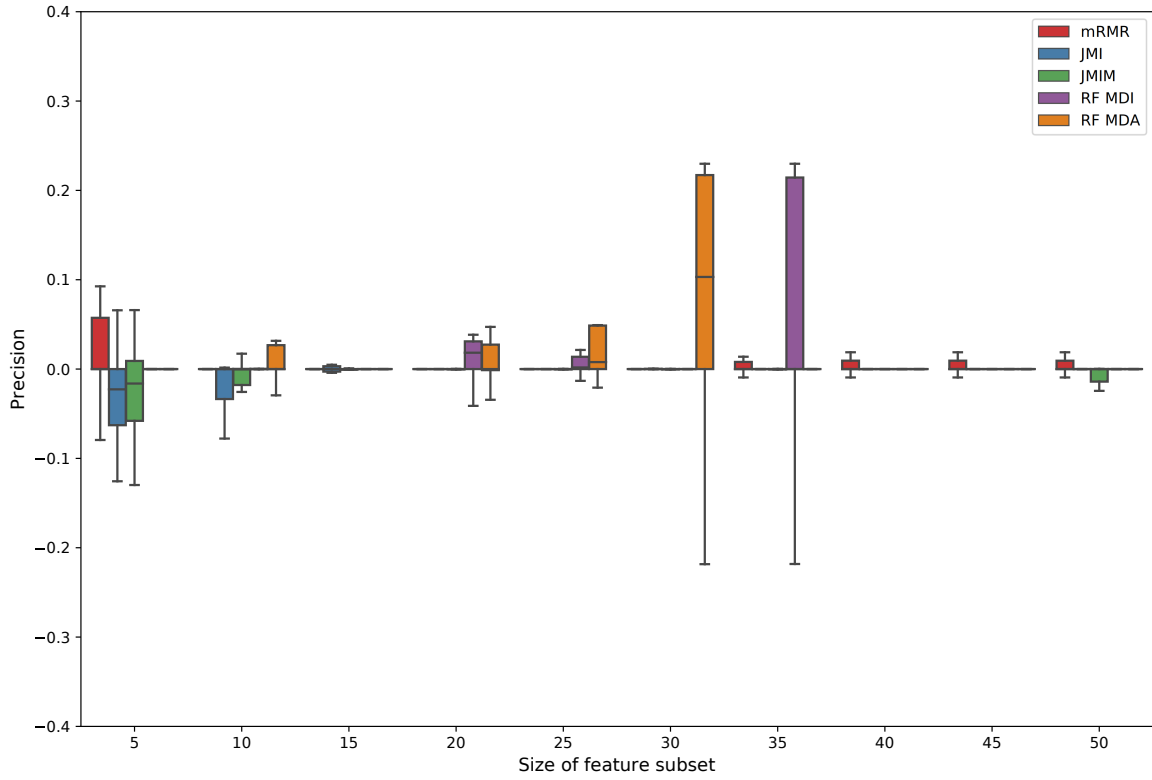


Figure 10: Boxplots of precision, here defined as the decrease in classification accuracy for networks with $n_o = 1000$ nodes when using networks with $n_s = 500$ nodes (rather than n_o nodes) for feature selection. The top and bottom graphs refer to the use of a 10-nearest neighbors and SVM classifiers, respectively. These graphs relate to the DMC versus DMR model selection problem in 50 replicate analyses.